GEOSPATIAL ANALYSIS OF SOLAR PHOTOVOLTAIC SUITABILITY

FOR SOLAR PHOTOVOLTAIC FARMS (SPVF)

by

ALEXANDER L. Y. DEVINE

(Under the Direction of Marguerite Madden)

ABSTRACT

Geospatial technologies including geographic information systems (GIS) and Lidar (Light Detection and Ranging) are increasingly being used to provide detailed and accurate spatial information for a variety of environmental analyses. One such application is site suitability analyses for Solar Photovoltaic Farms (SPVF), broad-scale systems designed to provide solar power to the electricity grid. The highly accurate representations of ground terrain conditions using digital elevation models (DEMs) derived from Lidar are critical for SPVF site suitability. However the expense associated with collecting aerial Lidar may not provide sufficient return on the investment for this particular analysis. A detailed comparison of Solar Photovoltaic (Solar/PV) site suitability analysis results performed with Lidar-derived 1.22-meter DEM vs. USGS NED 10-meter DEM will address that question. The results from this comparison will potentially inform decision-makers on the need for acquiring Lidar data in a region when investigating the siting of a SVPF installation.

INDEX WORDS: Geospatial, Solar, Solar Farms, AHP, DEM, Photovoltaic, Lidar, Site Suitability

GEOSPATIAL ANALYSIS OF SOLAR PHOTOVOLTAIC SUITABILITY FOR SOLAR PHOTOVOLTAIC FARMS (SPVF)

by

ALEXANDER L. Y. DEVINE

AB, University of Georgia, 1997

A Thesis Submitted to the Graduate Faculty of The University of Georgia in Partial Fulfillment of the Requirements for the Degree

MASTER OF SCIENCE

ATHENS, GEORGIA

2015

GEOSPATIAL ANALYSIS OF SOLAR PHOTOVOLTAIC SUITABILITY

FOR SOLAR PHOTOVOLTAIC FARMS (SPVF)

by

ALEXANDER L. Y. DEVINE

Major Professor:	Marguerite Madden
Committee:	Thomas Jordan
	Lara Mathes

Electronic Version Approved:

Suzanne Barbour
Dean of the Graduate School
The University of Georgia
August 2015

DEDICATION

This work is dedicated to my family: my mother, Rebecca DeVine, and my father, Dr. Jerry W. Devine, for their instilling in me a love of learning and encouraging perseverance, my wife, Anne Meyers DeVine, for her support and encouragement and my children, for inspiring me to become a better person.

ACKNOWLEDGEMENTS

I would especially like to acknowledge the support, encouragement and council of my committee, who helped me to develop this work. I would like to thank Lara Mathes in her help in developing the initial thesis concept. I would like to thank Jessica Cook Hale for her assistance with statistics and general encouragement. I would like to thank Anne, Meyers DeVine, Al Dixon and others for generously offering to proofread during the process: an offer I should have taken them up on. I also want to thank everyone who said, in some way or another, “Good for you” or “Don’t give up”, or “You are almost there!” when the process seemed weighty. This especially applies for Marguerite Madden, whose patience, kindness and understanding while this work unfolded for me was incredible.

TABLE OF CONTENTS

Page

LIST OF TABLES

Page

LIST OF FIGURES

Page

LIST OF EQUATIONS

CHAPTER 1

INTRODUCTION

Overview

A little over 60 years ago, at Bell Laboratories, a new technology was born with the creation of the first photovoltaic (PV) solar cell. According to Green (2000), "Photovoltaics involve the direct conversion of sunlight into electricity in thin layers of materials with properties intermediate between those of metals and insulators." Since its invention, this technology has increased in efficiency in that conversion of light to electricity and has become more widespread.

Many factors are driving down the cost of implementing solar/photovoltaic technology these days. More and more, governments, corporations and individuals are making the investment to tap in to this renewable, practically unlimited resource (Bazilian, et al., 2013). Even with declining start-up costs, there is significant interest in determining: 1) the benefit of these systems in a potential site before making a commitment; and 2) selecting a site that is appropriate. This is where solar site suitability analysis using geospatial techniques comes in to play.

A solar site suitability analysis is a formal process of defining factors that would impact whether a solar installation would be appropriate for a particular location and using those factors to make decisions concerning site selection. Depending on the type of installation,

there are certain criteria including distance from sufficient electric transmission lines, slope and aspect of the site, that, when analyzed together in a meaningful way, can help an interested party make the decision on that investment. This type of land-use analysis is often driven by spatial data, such as in landscape, urban and environmental planning. (Pereira, et al., 1993; Malczewski, 1999; Malczewski, 2004).

Spatial suitability analyses are often structured as a Multi-Criteria Decision Making (MCDM) process. MCDMs are, quite literally, the consideration of multiple criteria in the decision making process. One of these processes is the Analytic Hierarchy Process (AHP) created by Thomas L. Saaty of the University of Pittsburg (Saaty, 1990) With the AHP, the investigator simplifies a complex problem into pairwise evaluations of weighted criteria against each other. (Saaty, 1990) The criteria, in this case, are all the factors being considered that determine the suitability for a SPVF. Some examples of these criteria are slope (flat land is more ideal), aspect (southerly directions of sloped land are better) and distance from electric transmission infrastructure sufficient to carry the electricity produced.

In this study, the result of the decision-making process will be land that is ranked by its suitability to contain a solar installation: more specifically, a Solar Photovoltaic Farm (SPVF). SPVFs (also known as solar plant, solar ranch or solar power station), are broad-scale photovoltaic solar installations ranging anywhere from less than 5MW of electricity production on less than a hectare to 579 MW in the case of the Solar Star Projects in California that cover over 1300 hectares (DiSavino, 2014). These installations are

intended to supply power to the electric utility grid, rather than to specific structures or facilities.

These SPVFs are made possible by the development and advances in photovoltaic cell technology. Advances in understandings about the physics of light and energy blazed the path for the creation of the first efficient solar cell in 1954. The technology has been evolving and efficiencies have been increasing ever since (Green, 2000; Pearce, 2002, Pérez-Higueras, et al., 2011; Bazilian et al., 2013; Liang, et al., 2015).

The processes for determining site suitability for SPVFs have been established. However, there is still the question of spatial resolution requirements for the data used as input to geospatial suitability models such as MCDMs. Details of the characteristics of the earth's surface that influence the exposure of SPVF panels to sunlight, such as slope and aspect, have significant impact on site selection in an area being considered for siting a SPVF. Because of this, the spatial resolution of that data is important because data of high spatial resolution and small ground area coverage of individual pixels typically are more costly to acquire, manage and process. For example, the common spatial representation of the earth's surface is a Digital Elevation Model (DEM). A DEM is:

> "The representation of continuous elevation values over a topographic surface by a regular array of z-values, referenced to a common datum. DEMs are typically used to represent terrain relief." (Wade, 2006)

There are three main ways DEMs are produced: auto-correlated or manually interpreted from aerial photography, interpolated from elevations obtained from previous survey data or from electronic sensor systems that are either active or passive (Caruso, 1987). Many of the older technologies used to generate DEM data have limitations that lead to DEMs that have 30-meter to 10-meter resolutions. Newer methods can produce DEMS 5-meters and better. One of the prominent technologies from which high-resolution DEM data is produced today is Light Detection and Ranging (Lidar) (Rayberg, et al., 2009).

Lidar uses laser pulses to determine distance from reflective surfaces by measuring the travel time of the pulse from emission to return. Fig. 1-1 depicts the Lidar collection process:

Fig. 1-1: Lidar Collection Example

(Image source: http://www.sbgmaps.com/lidar_technologies.htm)

This image illustrates a scanner mounted on a plane that emits the laser pulses. The airborne platform not need be an airplane, as helicopters and unmanned aerial system technology are also used to collect Lidar data. A survey device that produces the energy that is measured is referred to as an “active” scanning device. The travel-time and trajectory of the pulse reflected returns are used to calculate the position the reflector represents relative to the GPS coordinates of the plane in its flight path at the time the pulse is emitted and received. Raw Lidar data are a collection of X, Y, Z points, often referred to as a “point cloud” that represent objects and surfaces that reflected the laser pulse.

Lidar can provide an accurate and detailed representation of the surface it encounters. Lidar, or Light Detection and Ranging, or Laser Detection and Ranging, is:

> “a mature mapping technology in the same company as radar and sonar. Airborne lidar mapping systems provides 3D information for the surface of the Earth which includes terrain surface models, vegetation characteristics, and man-made features. Lidar is an active sensing technology, i.e., it generates its own pulses of light and detects the reflections from those pulses (very similar to radar and sonar). (Renslow, 2012)

The acquisition of Lidar data from an altitude of 2000 meters can result in a point cloud of 1.0 points per square meter and be complied to meet a +/- 1 meter horizontal accuracy and a vertical accuracy of +/- 15cm (NOAA\GADNR, 2012). While this level of

accuracy and detail are desirable for many types of analyses, there is certain level of expense in collecting Lidar data which will be described in more detail later. The accuracy that Lidar can provide has found multiple applications across many disciplines (Wehr and Lohr, 1999), but is this level of detail worth the monetary investment in determining site suitability for SPVFs? Costs of Lidar acquisition are seeing a downward trend, but still are significant enough to potentially cause policy makers to ask whether the expenditure is necessary. In 2009, Sanborn Mapping quoted the Virginia Base Mapping Project $183/sq, km ($475/sq. mile) for a 1-meter point spacing Lidar survey and delivery of a bare-earth DEM for a 518-1295 sq. km. (200-499 sq. mile) area. Fugro Earthdata, Inc. estimated in 2011 that would be $135 to $175/sq. km. ($350 to $450/sq. mile) for the same information for a 259-1295 sq. km. (100-500 sq. mile) survey area. In 2013, the state of Michigan received estimates of approximately $58/sq. km ($150/sq. mile) for a similar product in a 259-1295 sq. km. (100-500 sq. mile) survey area. Even with this downward trend, should the most recent estimates hold that would still represent a cost for the 313 sq. km (121 sq. mi) area of this project at more than $18,000.

Despite these trends, Lidar acquisition remains a significant investment. If Lidar survey data are currently not available in an area being evaluated for the solar potential for its residents, decision makers may want to know just how much benefit it provides to solar/PV potential site surveys for SPVFs. This study will shed light on whether the detail and accuracy Lidar can provide is necessary to determine site suitability for SPVFs.

Problem Statement

The development of Solar Photovoltaic Farms (SPVF) is getting less expensive and efficiencies of photovoltaic cells are increasing, making this an increasingly viable and popular alternative solution to the energy needs of our country (Bazilian, et al, 2013). Innovative Solar Systems estimates the cost for installing SPVFs at $1,235,500/hectare ($500,000/acre) in the United States. Those interested in determining the best placement of these installations, maximizing their benefit or determining whether to make the investment at all will often perform or contract a solar suitability analysis. Especially when covering larger areas, these analyses utilize geospatial, or geographic information systems (GIS) data and modeling capabilities (Malczewski, 2004).

The remote sensing technology Lidar (Light Detection and Ranging), is enabling a marked increase in the accuracy and detail of some of the data used in land-use suitability and a myriad other types of analyses (Wehr and Lohr, 1999). An active Lidar sensor emits pulses of light energy that the time that it takes to reflect the energy, and the order of the return indicate the position of the reflector on the ground. By order of the return, it is meant that the light pulse will reflect off the first thing it encounters, but can also travel through non-solid reflectors such as tree canopy. The last return to the sensor, if not from a man-made object, is “bare-earth”. An aerial Lidar survey can vary in the post-spacing, or the average number of points measured in a given area. This can be as few as one every few square meters or 8 or more per square meter. When the post-spacing is around one point measured every square meter that is sufficient to generate a reliable 5-meter DEM and 2 foot contours from that. Do we always need this 5- meter and better DEM

level of detail in order to obtain desired results in determining site-suitability for SVPFs? For a typical site suitability study of a SPVF, is the benefit of Lidar enough to justify the cost of obtaining it if it is not already available?

Scope

The purpose of this quantitative study is to perform large-area Solar Photovoltaic Farm site survey analyses using DEMs of two different spatial resolutions and statistically compare the results in order to determine if the results are statistically similar enough to be considered "the same". The two analyses will utilize the same types of data, but one will substitute high-resolution elevation data typical of what can be derived from an aerial Lidar survey. More specifically, a 10-meter resolution United States Geological Survey (USGS) National Elevation Dataset (NED) DEM that is publically available at no cost will be used to derive slope and aspect of the land to inform one analysis, while a 1.22-meter Lidar-derived DEM, and derived slope data will inform the other. The 10-meter DEM is derived from 1:24,000 scale cartographic contours and is the predominant source in the NED. The influence of the variables (aspect and slope derived from the different resolution DEMs) will be assessed by repeating the process with the aspect and slope value having more weight in the decision making process. Other data in the analyses, such as road centerlines and hydrology, will remain constant for control.

The analyses is typical of previous MCDM SPVF site suitability surveys performed as informed by the literature (Gastli, 2007; Carrion, et al. 2008a; Carrion, et al. 2008b; Charabi and Gastli, 2011; Janke, 2010; Sanchez-Lozano, et al., 2013; Uyan, 2013). The

specific study that will be emulated is Melvut Uyan's "GIS-based Solar Farms Site Selection Using Analytic Hierarchy Process (AHP) in the Karipinar region, Konya/Turkey" (Uyan 2013). Uyan used elevation data derived from the Shuttle Radar Topography Mission (SRTM) at a resolution of 30-meters for an analysis that covered 6035 square kilometers. The criteria used by Uyan were modified slightly in the values of the sub-criteria to better suit this project and the addition of the aspect of the land as a criteria.

The location of the study is Athens-Clarke County (ACC), located in northeast Georgia within the Piedmont Physiographic Province (Fig. 1-2 and Fig. 1-3). The Piedmont is typified by mountainous area with hills and plains as well. Athens-Clarke County is more of the hill-and-plains-type piedmont geography with an average elevation of 194 meters (636 feet) above sea level. The region enjoys 218 days of sun per year, on average. This county has many advantages for this study including ready access, reasonable size of 306.137 sq. km (118.2 sq. miles), and a mix of urban, suburban and rural areas. If one were to have visited the USGS website (http://ned.usgs.gov/) and utilized the National Map Viewer and Download Platform (http://viewer.nationalmap.gov/viewer/) at the time of this study, the highest resolution DEM for Athens-Clarke County, GA is the U.S. Geological Survey (USGS) National Elevation Dataset (NED) ⅓ arc-second (10-meter) product. A county-wide aerial Lidar survey was made available to ACC in 2013 at a dramatically reduced cost due to NOAA already having a scheduled flight in the area and ACC adding terrestrial Lidar and orthophotos to the scope of that work. ACC's portion of

the cost was less than $100,000. Without the knowledge of the existence of the Lidar data, a researcher may question if the resolution of the 10-meter DEM was sufficient.

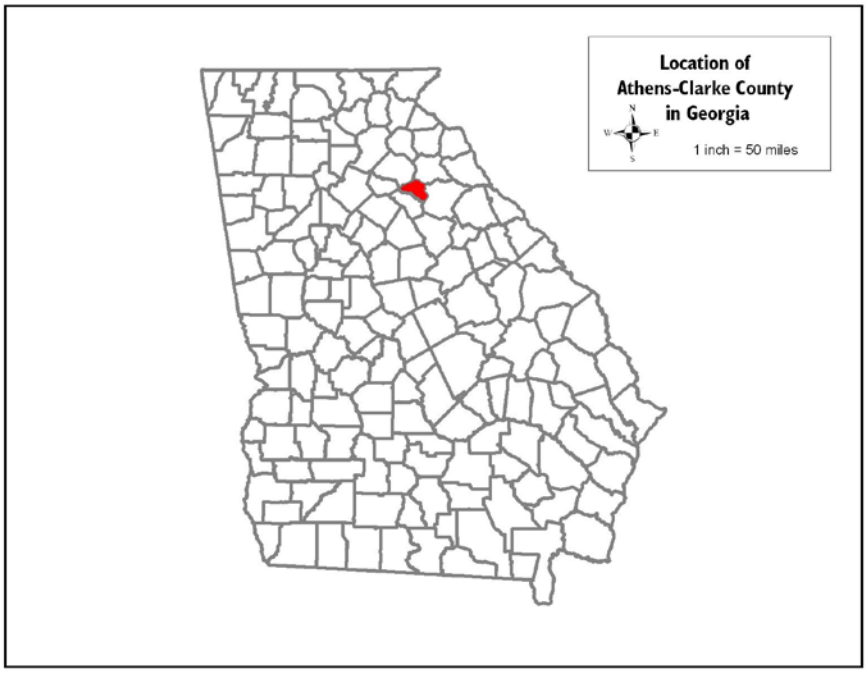

Fig. 1-2: Location of Athens-Clarke County in Georgia

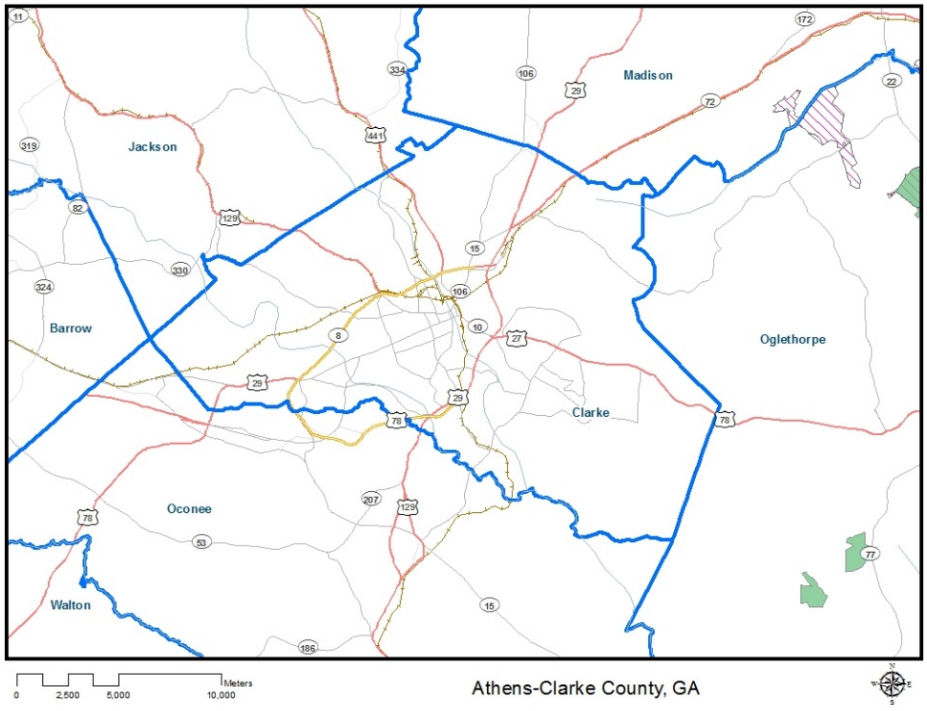

Fig. 1-3: Athens-Clarke County, Georgia

Background

In the past, there has been a widely-held misconception that solar power is only practical in the most sun-drenched of locales (Pearce, 2002). While there is certainly a benefit for placing solar arrays in such places, improvements in solar/PV technology has made installation of solar infrastructure practical and beneficial in areas previously thought not to have abundant solar resource. For example, Germany, has enjoyed 6.2% to 6.9% of its national electric power in 2014 produced from solar (Burger, 2014).

There are many types of "solar" power installations. The three main types are Photovoltaic (PV) arrays, Concentrated Solar Power (CSP) and Solar Thermal (REF). Photovoltaic arrays that use solar/PV cells in a solar panel to directly convert solar energy to electricity. Solar power systems concentrate solar energy using mirrors or lenses into a heat engine system to generate electricity. Solar thermal systems channel solar heat energy for heating, cooling and electricity generating applications. In this study, I will be focusing on Solar/PV-type systems in a Solar Farm.

Solar/PV systems rely on the photovoltaic cell to generate electricity. The efficiency of this technology has been increasing since it was developed and the relative cost has been decreasing (Pérez-Higueras, et al., 2011). The first solar cell was developed at Bell Laboratories in 1954. The efficiency of converting solar energy to electrical energy for that cell was 6%. In 2003, Goetzberger et al. (2003) published that the best laboratory

efficiency for single crystal silicon as 24.5%. Subsequently, advances in the cell itself and configurations to maximize exposure and boost efficiency of the cell have generated efficiencies approaching 50% (Liang, et al., 2015). As these efficiencies have been increasing, costs have been on the decline. One measure commonly used for PV solar arrays is $/Watt. In China, in 2006, one would pay roughly $4.5/Watt. In 2011, that had fallen to under $1/Watt (Bazilian, et al., 2013). In the U.S., the reported pricing for SPVFs that were completed in 2013 were around $3.00/Watt. Quotes on pricing in late 2012 for projects slated to begin installation in 2013 were around $1.92/Watt. In late 2014, quotes for modelled systems were averaging around $1.80/Watt. In fact, between 1998 and 2013 the system prices on residential and commercial systems declined 6-7% per year and by 12-15% from 2012 to 2013 (Barbose, 2014).

Solar/PV system's sizes and types range from broad-scale solar farms down through large building installations to systems for use by residential home-owners. Each of these systems has site selection criteria that define their suitability and have some overlap, but the scales and desired criteria of the system are distinct enough to require specific types of suitability analysis.

The Solar Farm, also called PV power stations or solar park, is a PV system designed to generate direct current (DC) electricity to supply to the electricity grid, after conversion to alternating current (AC) electricity. These solar farms can implement solar panels that are in a fixed position or also track the sun as it crosses the sky (at greater initial and maintenance costs). SPVFs require a significant amount of land (between 1 and 100

acres) with some adjacency to power lines sufficient to carry the average of 6.9 MegaWatts each acre of installation can produce (Ong, et al., 2013). Among other criteria, areas with low slope, southerly aspect and low land cover are better suited for solar farms. This leads one to think SPVFs should be sited on rural lands along major roads which typically have higher-capacity power lines along them. While this is generally true, there is also increased interest in solar farms sited in expansive parking lots to generate electricity and provide shelter for the vehicles at the same time (Birnie, 2009). Utilizing municipal capped (decommissioned) landfill, or brownfield, areas is also a popular area of exploration (Adelaja, et al., 2010).

Performing the type of large-area analysis required to determine where to site these SPVFs is possible through use of spatial analysis. The potential resolution of elevation data in these analyses was increased dramatically by the commercial emergence of Lidar surveying in the 1990s (Yan, et al., 2014). Lidar first gained widespread public attention after the attacks on 9/11 when it was used to map Ground Zero to provide an accurate digital model for rescue and recovery operations. Since that time, prices for acquiring Lidar have declined and many regions have performed surveys and the USGS has created the 3D Elevation Program to provide a clearinghouse for all of this data. (Neal, 2015) Before the increased availability of aerial-based Lidar survey data, solar photovoltaic deployment optimization surveys used the data that were available: infrastructure and land cover/land use information based on aerial photography and elevations from lower-resolution remotely-sensed data such as the Shuttle Radar Topography Mission V2 (SRTM V2 – 90-meter), Advanced Spaceborne Thermal Emission and Reflection

Radiometer Global Elevation Model (ASTER/GDEM – 30-meter) and the lower resolution NED (30-meter). More recently, certain areas enjoy being part of a bi-monthly updated 10-meter and 3-meter NED survey. There is also the USGS 3D Elevation Program (3DEP). 3DEP is a national program managed by the USGS to acquire high-resolution elevation data, including Lidar data. The Lidar data used in this study is in 3DEP. For areas that do not have access to the 3-meter resolution NED data, there is a large span between that and the resolution of the DEM that can be produced from an aerial Lidar survey, which, with 1.5-meter post-spacing (distance between Lidar sample points) can be 3 meter or better (Heidemann, 2012).

Significance

The cost of implementing solar/photovoltaic (PV) technology is decreasing and, at the same time, the efficiency of photovoltaic technology is improving**.** With this being the case, it logically follows that there may be an increased interest in investment into solar technology installations. These installations may be in the form of a Solar Farm, a broad-scale rooftop array or even residential rooftop panels. Siting of these installations is typically informed by spatial data. With aerial Lidar surveys allowing for the broad-scale acquisition of very detailed elevation and surface models, decision makers considering these solar options may want to know if it is worth investing in a Lidar survey. While this may not be practical for individuals curious about their home's potential, private and government entities might be interested to learn about the return on the investment of an aerial Lidar survey and its impact on solar site suitability surveys.

CHAPTER 2

REVIEW OF LITERATURE

Overview

Before 2008, there was little mention of Lidar data in the literature concerning the process of assessing solar/PV site suitability. A real explosion in the use of Lidar in the process occurred in the early years of this decade (2010-2015). In fact, in recent years, Lidar's impact on environmental modelling was nothing short of revolutionary (Schwarz, 2010). Lidar was being used to not only generate accurate base data, such as digital elevation models, but also to derive data sets such as detailed infrastructure, capable of informing the site suitability analysis process to levels that were previously unobtainable. What is missing from the current literature, however, is a focus on quantifying the benefit of using Lidar to inform solar/PV site suitability analysis. Since Lidar survey data on a large-scale (i.e., fine-scale) is not available in all areas and is typically expensive to acquire, the added value of using Lidar data to assess environmental variables for siting solar/PV farms should be evaluated.

Solar/PV Technology:

In this same time period that Lidar technology made advances in environmental modeling, the technology of solar photovoltaics changed rapidly, too. Some improvements were made to the solar cell itself. An example of this is that the efficiencies of multi-junction cells have reached 44.7%. These type of cells are where the

solar cell has multiple interfaces with the semiconductor materials in a concentrator system. For comparison, this is an improvement from roughly 16% efficiency when this particular cell technology was developed in 1983 (Kasmerski, 2010).

Other developments in solar technology focused on improvements in the photovoltaic array. One of these is Concentrator PhotoVoltaics (CPV), where optical systems concentrate solar energy onto the solar cells (Pérez-Higueras, et al., 2011). Another of these system improvements is the hybrid PhotoVoltaic/Thermal (PVT) solar collector, where cooling systems improve the efficiency and lifespan of the solar cell (Makki, et al., 2015). Peak efficiencies of PV cells in a thermal system have been measured at 48% and represent an important achievement in solar/PV technology (Liang, et al., 2015). The trend in efficiencies, through improvements to the cell itself or the array, are upward while the costs of the technology is decreasing. An observation known as Swanson's Law states module prices reduce 19% for every doubling of cumulative volume (Swanson, 2006).

There are the realities and best practices to consider when discussing the installation of solar technology in the form of a SPVF. The National Renewable Energy Laboratory (NREL) recently published a best practices guide for the operation and maintenance guide for solar installations, including SPVFs (Keating, 2015). While SPVFs can be kept in good service for decades, there is potential for lost revenue and low energy generation with unmanaged issues. Sixteen major Operations and Maintenance (O&M) issues include: Perimeter fence damage, ground erosion, transformer leakage, inverter damage,

broken conduits, combiner box damage, vegetation overgrowth, cell browning/discoloring, panel shading, shorted cells, natural damage (from weather), vandalism, defective tracker, racking erosion, unclean panels and animal nuisance. An O&M agreement to mitigate these potential issues is strongly encouraged for SPVFs.

As a renewable resource, there is a desire and pressure for SPVF installations to be ecologically responsible. In the United States and Europe, many solar farm ecological and community best practices have been established in siting SPVFs. Some of these published by the United Kingdom's Solar Trade Association (Solar Trade Association, 2015) include utilization of environmentally sound sites, minimization of visual impact, community engagement in planning, sound ecological site stewardship, local sourcing of labor for installation and maintenance, encouraging site use for educational purposes and the return of the land to its previous use on end of project life.

Lidar Technology

The principle of Lidar has its roots in the 1930s when searchlight beams were used to try to measure air density profiles for meteorological purposes. When the laser was invented in 1960, the technology developed quickly and the first textbook on the subject was published in 1976. (Wandinger, 2005). The value of 3-dimensional point cloud data acquired by laser scanners mounted on aircraft was quickly realized for creating detailed DEMs, 3-D visualizations and terrain assessment for environmental modeling. of Lidar-derived 3D landscape features also enabled Land Use and Land Cover (LULC)

classification data directly from the aerial Lidar data with classification accuracies reported in the mid 90% range (Antonarakis, et al., 2008).

MCDMs & Solar-Suitability Studies

The general principles of land-use suitability analysis, as well as the problems and prospects of the technique are covered in great detail by Jacek Malczewski in his article "GIS-based land-use suitability analysis: a critical overview." (Malczewski 2006a). The process of land-use suitability analysis is, by nature, multi-criteria and is a natural fit for MCDM methods (Malczewski, 2006b). Specifically, energy and environmental modeling can benefit from these tools (Huang, et al., 1995).

A variety of recognized MCDM methods to obtain solar site suitability were detailed in the literature (Charabi and Gastli, 2011; Uyan, 2013), as well as papers on developing custom MCDMs for the purpose of determining SPVF site suitability (Joerin, et al., 2001; Carrión, et al., 2008). In some research, the MCDM was a combination of established MCDM methods that were either performed in detail (Charabi and Gastli, 2011) or utilized in the form of an ESRI-developed Spatial Analyst MCDM product (Janke, 2010). There were also comparisons of MCDM methods used for solar site suitability analysis (Sánchez-Lozano, et al., 2013). Aragonés-Beltrán, et al. (2010) explored using an Analytic Network Process to help make decisions on suitable sites for investment after the suitability was determined. One particular MCDM encountered with some frequency in regards to solar site suitability was Thomas L. Saaty's (1990) Analytic Hierarchy Process (AHP) (Charabi and Gastli, 2011; Uyan, 2013; Sánchez-Lozano, et al., 2013).

The prevalence of the use of AHP and other MCDMs in the literature for solar site suitability led to the use of the method in this study, in particular, the AHP method employed by Melvut Uyan in his study in the Karapinar region, Konya/Turkey (2013).

Remotely sensed data, such as aerial photography, satellite imagery and Lidar, are utilized to obtain data, such as road centerlines, slope, aspect, LULC, appropriate for the solar-suitability analysis to be performed (Hammer, et al., 2003). This, combined with soundly designed MCDM, can produce an effective result for an analysis by providing not just a boolean result of "yes or no", but facilitates a suitability model that allows categorization of ranked suitability (Carrion, et al. 2008a; Carrion, et al. 2008b; Charabi and Gastli, 2010; Janke, 2010; Sanchez-Lozano, et al., 2013; Uyan, 2013).

Criteria for Solar-Suitability Studies

When discussing suitability studies for solar installations, one must first consider the solar resource itself. The solar resource is a measure of the solar energy that reaches areas on earth based on solar, geographic and meteorological data (Myers, 2005; Renné, et al., 2008). This type of data is readily handled in a GIS (Sorenson, 2001). One can easily obtain this spatial solar resource data from the National Renewable Energy Lab at a 10-kilometer resolution. The model used to generate this data includes:

> "...hourly radiance images from geostationary weather satellites, daily snow cover data, and monthly averages of atmospheric water vapor, trace gases, and the amount of aerosols in the atmosphere to calculate the hourly total insolation (sun and sky) falling on a horizontal surface." (Perez, et al., 2002)

Those without access to the existing data for solar resource will sometimes develop their own methods to obtain resource data in order to perform solar farm suitability analysis (Gastli and Charabi, 2010). The solar resource in a smaller project area, such as the one in this study, may not vary enough to be significant in determining site suitability within the study area, but will certainly inform estimates of potential electrical production of sites identified by other criteria (Uyan, 2013). While there is no size minimum for what can constitute a SPVF, some companies involved in installation have set minimums of 2-4 hectares (5-10 acres) for their individual threshold for beginning to profit from "economies of scale".

Two drivers for suitability of a SVPF are the slope and aspect of an area. In order to utilize the solar resource, the panels in an array should ideally be located to maximize solar exposure. If land is too sloped, the solar panel arrays will potentially cast shadow on each other during the day. If an area, even with low slope, has an undesirable aspect, this can reduce the efficiency of an array placed on such land. Slope and aspect of the land surface is typically derived from a DEM. The importance of slope and aspect to the site suitability analysis process is fundamental to the question posed by this research.

There are many other considerations when performing a SPVF site-suitability survey. One particular concern is the impact that the installation of a SPVF has on the ecology of an area (Stoms, et al., 2013). This study will include typical ecologically sensitive areas such as wetlands and riparian zones in the MCDM to inform the analysis. There are also aesthetics to consider. One might establish a buffer distance from residential areas where

the Not In My BackYard (NIMBY) or Locally Undesirable Land Use (LULU) effects may be a factor (Joerin, et al., 2001; Janke, 2010). The proximity to power grid infrastructure sufficient to carry the power generated by the SPVF is also a factor.

There are additional cutting-edge uses of Lidar that can inform the SPVF suitability analysis. For example, when defining a potential area on which to develop a SPVF, one might desire to keep the tree cover on the edges of your site, or perhaps the trees are part of a riparian or wetland area that cannot be disturbed. This is where an analysis that includes vegetation structure details and light diffusion caused by the tree canopy is useful. By combining Lidar and GIS solar resource information, one can model the solar potential even of subcanopy. (Bode, et al., 2014). Additionally, one can use Lidar to map subcanopy solar potential over the days across the year (Peng, et al., 2014). While the inclusion of these newer sort of data in solar site suitability analysis is outside of the scope of this study, this level of detail for assessing SPVF site suitability is a further indication of the power of Lidar data and the potential complexity of the analysis for site-suitability.

While Lidar may arguably benefit the analysis for the siting of SVPFs, the expense of obtaining the data is often prohibitive. Either the budget or the scope (or both) of the project can be a factor in deciding if LiDAR should be incorporated in SPVF suitability analysis. In either case, methods that do not specifically involve data derived from Lidar to achieve results have been used. The method developed by Charabi and Gastli (2010) to reveal the solar prospects in Oman (119,499 sq. miles) was developed without the benefit

of Lidar due to the large area involved. This also was true in a case study in Fujian Province (46,873 sq. miles)(Sun, et al., 2013). None of this is explored with the idea of attempting to diminish the value of Lidar, in general. Lidar technology is allowing new types of research to be performed and has potential for continuing to facilitate similar advances in the future.

On reviewing the literature, other comparison studies, in the same spirit of the one being proposed, were encountered. Studies were found comparing the effect on analysis of Lidar-derived DEMs to other types of DEMs in a variety of applications, such as: forestry (Hummel, et al., 2011), hydrology (Haile and Rientjes, 2005; Murphy, et al., 2008; Yang, et al., 2015), soil mapping (Shi, et al, 2012) and geomorphology (Vaze, et al., 2010), to name a few. One study by Rayburg, et al., (2009) focused on a direct comparison of Lidar-derived DEM to a Differential GPS-derived DEM and a 9" DEM of Australia, while another used a Lidar DEM as a control for assessing the accuracy of another DEM (Dehvari and Heck, 2012). While there are studies comparing Lidar-derived DEMs to other sourced DEMS, there is nothing encountered in the literature that poses the question proposed in this study specific to site suitability for SPVFs. This study therefore makes a contribution to the SVPF modeling literature by filling that gap.

CHAPTER 3

MATERIALS & METHODOLOGY

Overview

Primarily, this study involves the performance of two complete MCDM SPVF Site Suitability Analyses similar to those performed by Melvut Uyan in his study in the Karapinar region of Turkey (Uyan 2013). Each of these analyses were performed using aspect and slope values ultimately derived from DEM sources of 10-meter and 1.22-meter resolution. Statistical analyses were performed on the source, intermediate and final data to determine correlation and deviation from each other due to the resolution differences of the source DEMs. Secondarily, to test the influence of AHP weights on the analyses, each of these two analyses were repeated with additional "Passes" where the importance of the slope and aspect variables are increased in the AHP.

In performing this study, criteria for what defines suitable land for an SPVF were determined. Criteria of slope, aspect, distance from residential areas, LULC, distance from roads and distance from transmission lines of sufficient capacity were used. Although not used by Uyan (2013), aspect was added to the analysis as it has been found to be important to the decision making process for solar site suitability (Carrión, et al., 2008a; Sánchez-Lozano, et al., 2013). Solar resource is not being considered as a factor in the AHP, as the range of the value in the study area is 4.55 to 4.6 kWh/sq.m/day. This is not surprising, given the relatively small area of the study. While the solar resource

data was not be used in the AHP, it was used to generate estimates of electric power potential from results of the analysis. Additionally, a report for results obtained using 1.22-meter DEM vs. the 10-meter DEM data.for three sites identified by the analyses as highly suitable for SPVFs was generated in order to compare the utility of Lidar-derived terrain characteristics.

Software & Resources

Analysis and production of GIS data were performed using ESRI ArcGIS Desktop 10.1. Klaus D. Goepel's "Online BPMSG AHP Priority Calculator" was used to develop the AHP. Statistics were generated using spatial statistics tools in ArcGIS Desktop, detailed when utilized.

Execution Plan

The execution plan for this project is provided in Fig. 3-1:

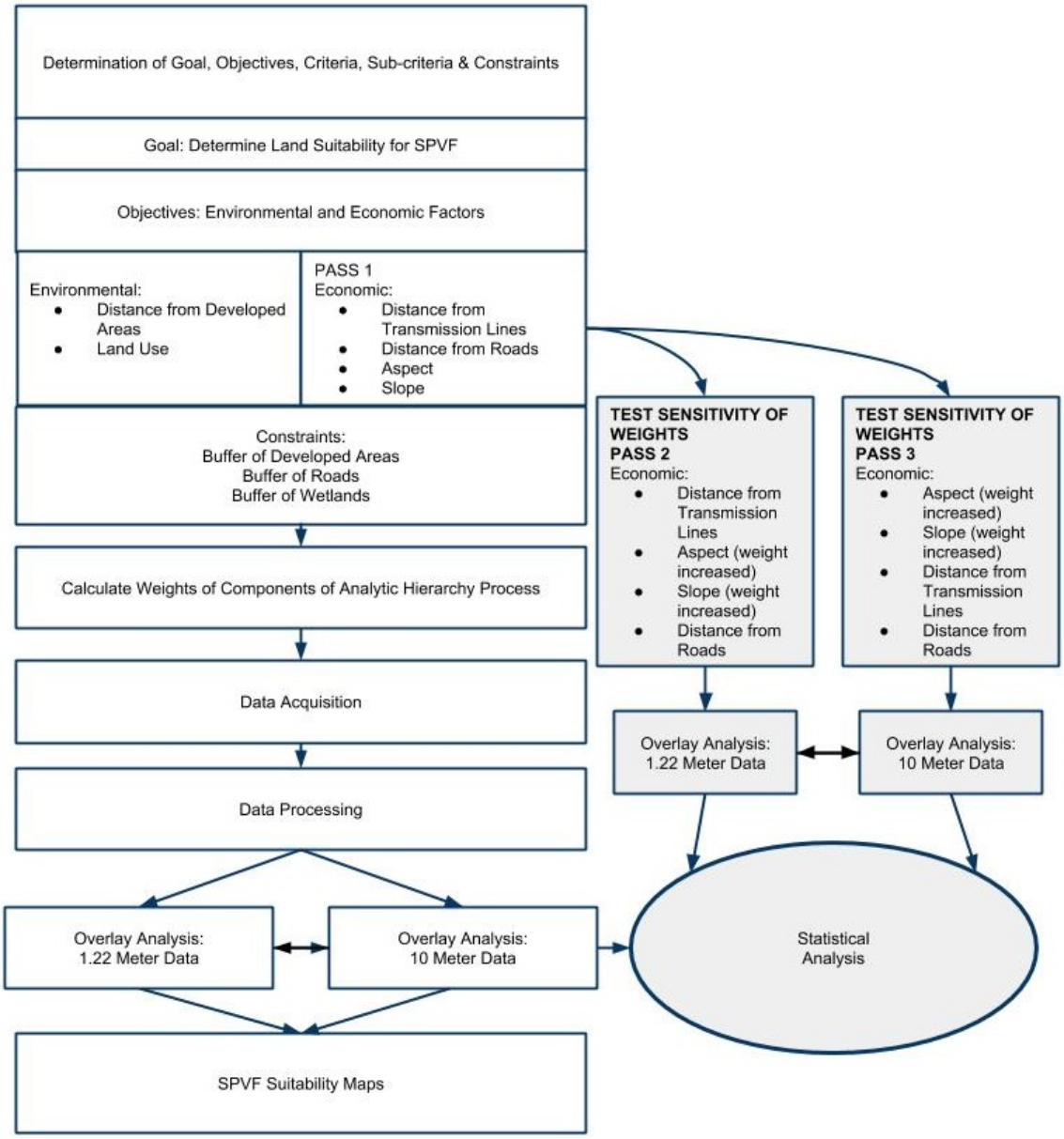

Fig. 3-1: Execution Plan for Project

Development of AHP Structure

In order to utilize AHP in the decision-making process for the generation of the SPVF Suitability Maps, the Objectives, Criteria, Sub-criteria and Constraints were established. Each of these terms has a special meaning in the process. The Goal is the determination

of suitability itself. The Objectives, in this case, are the main factors that determine that suitability and are divided into environmental and economic factors which are weighted and summed to represent the Goal. The Criteria are the properties of the Objectives that are weighted and overlain to determine the Objectives value. The Sub-criteria are the properties of the Criteria that are weighted and overlain to determine the Criteria value. The constraints are areas of zero suitability and were removed from the final data to produce the suitability maps.

In anticipation of the development of the AHP, the relative importance of each Objective, Criteria and Sub-criteria to each other were established. This was accomplished by using the AHP evaluation scale of 1 to 9 by 1. This means that the scale is a ranking from 1 to 9 and the scale unit is 1. This is shown in Table 3-1.

Table 3-1: AHP Evaluation Scale

Numerical Value of P_y	Definition of Value
1	Equal importance of i and j
3	Moderate importance of i over j
5	Strong importance of i over j
7	Very Strong importance of i over j
9	Extreme importance of i over j
2,4,6,8	Intermediate values

For example, the LULC data was consolidated into categories useful to the AHP process and then the relative importance of the different LULC classifications was established, as shown in Table 3-2.

Table 3-2: EXAMPLE - AHP Comparison for Land Use/Land Cover Criteria

	Barren	Shrubland	Herbaceous	Forest
Barren	1	2	3	7
Shrubland	0.5	1	3	6
Herbaceous	0.33	0.33	1	5
Forest	0.143	0.167	0.2	1

In the case of the LULC comparison, this difference in importance can be interpreted as whether there are policies or economic factors in effect that encourage or prohibit a specific land LULC from being used for a SPVF. The Barren land was considered most appropriate for using as a SPVF with a score of 1. The Shrubland was considered to only be slightly more suitable than Barren land, with Barren considered a 1 on the 1 to 9 by 1 scale and Shrubland a 2. Herbaceous land was considered a less important than both Barren and Shrubland, but Herbaceous was considered also less important than Shrubland. Forested LULC was considered the least suitable by a considerable factor due to environmental impact (and expense) of the clearing of a forested area for a SPVF. The rest of the Criteria, Objectives and the Goal value were developed in a similar fashion, detailed in the Appendix.

In Uyan's study, there was a mask of areas established to be zero suitability for SVPFs. These are referred to as Constraints. The specific constraints he uses include: 500 meters from residential areas, 100 meters from roads and, basically, on rivers, lakes, wetlands. The buffer from residential areas is to mitigate the NIMBY effect and avoiding potential obstruction to residential development. The buffer mask for roads is for aesthetics, as well, but siting SVPFs too far from roads can be negative due to an increase in construction costs. The buffer for rivers, lakes and wetlands is to protect the ecology of

those types of land covers and, in some cases, to respect ordinances formalizing such a buffer. In this study, the 100 meter distance from developed areas was established. The reduction is due to the relative proportion of developed areas in the Athens-Clarke County area make a 500m constraint buffer too restrictive. The 100 meter buffer from roads was maintained and the buffer for rivers, lakes and wetlands was established at 50 meters for lakes, wetlands and minor rivers and streams with a 150 meter buffer for major named creeks and rivers. This meets or exceeds recommendations of the U.S. Green Building Council and LEED Site Selection standards. These masks were applied using ArcGIS after the primary analyses are complete to effectively "zero out" the raster cells where an SVPF is not suitable.

With the relative importance for each of the components established on a 1 to 9 by 1 scale, and the constraints defined, the next step was to use AHP to calculate the weights for the analyses.

Calculation of Weights of Components of AHP

In order to take the comparisons established and generate weights from them, the comparisons were arranged in a matrix. Each column in the matrix is then summed. Each entry in the matrix is divided by its column sum. The values are averaged across the rows to obtain the relative weights (sum of weights =1). Table 3-3 provides an example using the pairwise comparisons for the Land Use/Land Cover data used in this study.

Table 3-3: LULC Matrix and Weights Example

Matrix	Barren	Shrubland	Herbaceous	Forest	
Barren	1	2	3	7	
Shrubland	0.5	1	3	6	
Herbaceous	0.33	0.33	1	5	
Forest	0.143	0.167	0.2	1	
					SUM of Weights
Weights	0.468	0.322	0.161	0.049	1.000

During the calculation of weights, the Consistency Ratio (CR) is calculated to control the consistency of the pairwise comparisons. The CR is computed by, first, calculating the eigenvector and the maximum eigenvalue (λ_{max}) of each matrix of a size *n* x *n* (in our example 4 x 4) size. The eigenvector of a square matrix is a vector that points in a direction which does not change under the associated linear transformation. Next, the Consistency Index (CI) is calculated with Equation 3-1:

Equation 3-1: Calculation of the Consistency Index

$$CI = (\lambda_{max} - n)/(n - 1)$$

Finally, the CI value for the matrix is checked against the Random Consistency Index (RI) to compute the CR with Equation 3-2:

Equation 3-2: Calculation of the Consistency Ratio

$$CR = CI/RI$$

When CR is less than or equal to 0.10, the degree of consistency is satisfactory. If the CR is greater than 0.10, the AHP results may not be valid. In our Land Use/Land Cover example, the λ_{max} is 4.139 and the RI for a 4 x 4 matrix is 0.9. The process yields a CR of 0.051, or 5.1%. This portion of the AHP is shown to be satisfactory.

The weights and CRs were computed for each of the three passes that were developed to test the sensitivity of the weights on the analyses. These results are summarized in Tables 3-4, 3-5 and 3-6:

Table 3-4: AHP Weights and CR Values - Pass 1

Goal	Objective - CR	Wt	Criteria (unit) - CR	Wt	Sub-criteria	Wt
Determine Suitability for SPVFs in ACC	Environmental Factors - 0.000	0.530	Distance from developed areas (m) - 0.040	0.250	< 100	0.000
					100 to 500	0.105
					> 500 to 1000	0.258
					> 1000	0.637
			Land use (type) - 0.051	0.750	Barren	0.468
					Shrubland	0.322
					Herbaceous	0.161
					Forest	0.049
					Wetlands	0.000
					Developed	0.000
					Open Water	0.000
	Economic Factors - 0.016	0.470	Distance from transmission lines (m) - 0.063	0.550	< 2000	0.657
					2000 to 3000	0.203
					> 3000 to 4000	0.094
					> 4000	0.046
			Distance from roads (m) - 0.040	0.250	< 100	0.000
					100 to 500	0.637
					> 500 to 1000	0.258
					> 1000	0.105
			Aspect (direction) - 0.049	0.100	Flat, S, SW or SE	0.636
					East	0.161
					West	0.161
					North, NW, NE	0.043
			Slope (%) - 0.043	0.100	< 5	0.565
					5 to 8	0.262
					> 8 to 10	0.118
					> 10 to 12	0.055
					> 12	0.000

Table 3-5: AHP Weights and CR Values - Pass 2

Goal	Objective - CR	Wt	Criteria (unit) - CR	Wt	Sub-criteria	Wt
Determine Land Suitability for SPVFs	Environmental Factors - 0.000	0.530	Distance from developed areas (m) - 0.040	0.250	< 100	0.000
					100 to 500	0.105
					> 500 to 1000	0.258
					> 1000	0.637
			Land use (type) - 0.051	0.750	Barren	0.468
					Shrubland	0.322
					Herbaceous	0.161
					Forest	0.049
					Wetlands	0.000
					Developed	0.000
					Open Water	0.000
	Economic Factors - 0.016	0.470	Distance from high-capacity transmission lines (m) - 0.063	0.520	< 2000	0.657
					2000 to 3000	0.203
					> 3000 to 4000	0.094
					> 4000	0.046
			Aspect (direction) - 0.049	0.200	Flat, S, SW or SE	0.636
					East	0.161
					West	0.161
					North, NW, NE	0.043
			Slope (%) - 0.043	0.200	< 5	0.565
					5 to 8	0.262
					> 8 to 10	0.118
					> 10 to 12	0.055
					> 12	0.000
			Distance from roads (m) - 0.040	0.080	< 100	0.000
					100 to 500	0.637
					> 500 to 1000	0.258
					> 1000	0.105

Table 3-6: AHP Weights and CR Values - Pass 3

Goal	Objective - CR	Wt	Criteria (unit) - CR	Wt	Sub-criteria	Wt
Determine Land Suitability for SPVFs	Environmental Factors - 0.000	0.530	Distance from developed areas (m) - 0.040	0.250	< 100	0.000
					100 to 500	0.105
					> 500 to 1000	0.258
					> 1000	0.637
			Land use (type) - 0.051	0.750	Barren	0.468
					Shrubland	0.322
					Herbaceous	0.161
					Forest	0.049
					Wetlands	0.000
					Developed	0.000
					Open Water	0.000
	Economic Factors - 0.016	0.470	Aspect (direction) - 0.049	0.360	Flat, S, SW or SE	0.636
					East	0.161
					West	0.161
					North, NW, NE	0.043
			Slope (%) - 0.043	0.360	< 5	0.565
					5 to 8	0.262
					> 8 to 10	0.118
					> 10 to 12	0.055
					> 12	0.000
			Distance from high-capacity transmission lines (m) - 0.063	0.200	< 2000	0.657
					2000 to 3000	0.203
					> 3000 to 4000	0.094
					> 4000	0.046
			Distance from roads (m) - 0.040	0.080	< 100	0.000
					100 to 500	0.637
					> 500 to 1000	0.258
					> 1000	0.105

Each pass shows the increase in the influence of slope and aspect on the AHP model. At Pass1, the total influence of aspect and slope is approximately 10% (20% of the Economic Objective which is roughly 50% of the Determination of Land Suitability for

SPVFs Goal), at Pass 2, the influence increases to 20 % of the model and at Pass 3 comprises 36% of the influence on the model. The CR values for the AHP development process was sound in all instances, which gave confidence in the consistency of the pairwise comparisons. With the AHP importance and weights for each of the components established, the next step was to gather all of the data for the analyses.

Data Acquisition

The processes of executing the analysis plan was begun by collecting the necessary data to create the suitability maps for the project. The data were from a variety of sources, indicated in their descriptions, and all data were reprojected, if necessary, to the following projection for analysis:

NAD 1983 NSRS2007 StatePlane Georgia West
FIPS 1002 Ft US
WKID: 3521 Authority: EPSG
Projection: Transverse_Mercator
False_Easting: 2296583.333333333
False_Northing: 0.0
Central_Meridian: -84.16666666666667
Scale_Factor: 0.9999
Latitude_Of_Origin: 30.0
Linear Unit: Foot_US (0.3048006096012192)

Geographic Coordinate System:
GCS_NAD_1983_NSRS2007
Angular Unit: Degree (0.0174532925199433)
Prime Meridian: Greenwich (0.0)
Datum: D_NAD_1983_NSRS2007
Spheroid: GRS_1980
Semimajor Axis: 6378137.0
Semiminor Axis: 6356752.314140356
Inverse Flattening: 298.257222101

Fig. 3-2: Project Geographic Projection

As the final analysis included estimating the solar potential of highly suitable areas for SPVFs, the National Renewable Energy Labs (NREL) Solar Resource Data was collected. These data represent the average solar energy exposure for an area in units of kWh/sq.m/day at a 10-km resolution. The value range for the data in the study area is 4.55 - 4.60 kWh/sq.m/day averaged over 1998 to 2009. This is a small range that effectively makes this a constant.

A Lidar-derived DEM was obtained for the study area. This 1.22-meter DEM (elevations in feet) was among the deliverables of the "2013 Lidar Survey for Athens Clarke County – Classified". This survey was a NOAA/GADNR/EPD developed Lidar point collection project for Barrow, Clarke, Madison and Oglethorpe Counties and was executed by PhotoScience, Inc. (now Quantum Spatial). The survey collected one point per sq. meter point spacing or better which was sufficient to produce the DEM at the resolution indicated. The LiDAR data were compiled to meet a 1 meter horizontal accuracy. The calibration of the LiDAR sensor itself and the calibration process of the data produced by this sensor ensure that this accuracy is met. The vertical accuracy of the data was 15.0 centimeters RMSE or better. The Lidar points were classified to American Society of Photogrammetry and Remote Sensing standards. The DEM data consisted of 211 tiles of 1,524 meters x 1,524 meters for the ACC area.

For the comparison a USGS NED ⅓ arc second (10-meter) DEM dataset was acquired. These data consist of seven DEM tiles: Nicholson_GA, Hull_GA, Statham_GA, Athens_west_GA, Athens_east_GA, Crawford_GA, Barnett_shoals_GA. Collected in

1998, elevation values were in meters and a z-factor of 3.28084 was applied during the re-projection process to convert elevation values to US feet to match the Lidar DEM values for analysis.

Another raster dataset acquired for this project was a regional portion of the National Land-Cover Dataset (NLCD). These data were derived from 30-meter Landsat Thematic Mapper (TM) imagery and have consistent land cover for the entire U.S. classified over a range of years using the NLCD Land Cover Classification System, revised in 1999. These classifications are indicated in Table 3-7.

Table 3-7: Level 2 NLCD Land Cover Classification System

Water
11 Open Water
12 Perennial Ice/Snow
Developed
21 Low Intensity Residential
22 High Intensity Residential
23 Commercial/Industrial/Transportation
Barren
31 Bare Rock/Sand/Clay
32 Quarries/Strip Mines/Gravel Pits
33 Transitional
Forested Upland
41 Deciduous Forest
42 Evergreen Forest
43 Mixed Forest
Shrubland
51 Shrubland
Non-natural Woody
61 Orchards/Vineyards/Other
Herbaceous Upland
71 Grasslands/Herbaceous
Herbaceous Planted/Cultivated
81 Pasture/Hay
82 Row Crops
83 Small Grains
84 Fallow
85 Urban/Recreational Grasses
Wetlands
91 Woody Wetlands
92 Emergent Herbaceous Wetlands

Vector data acquired included a county outline for clipping and cartographic purposes (ACC Planning Department, 2008). In order to develop additional criteria and constraints for our analyses the following vector data were acquired: road centerlines for ACC and surrounding counties (Georgia Department of Transportation, 2012), hydrology polygons (ACC Planning Department, 2008), hydrology arcs (ACC Planning Department, 2008) and wetlands (ACC Planning Department, 2008).

Data Processing

In order to prepare the data for analyses, a variety of geoprocessing tasks were applied. These processing tasks were primarily performed using ArcGIS 10.1 and, specifically, many of the processes were part of the ArcGIS Spatial Analyst extension. All of the processed data were clipped to the ACC boundary for consistency using the raster and vector Clip tools.

The Lidar and 10M DEM tiles were mosaicked into a raster mosaic dataset. Each DEM dataset was then resampled using the Resample tool. The 1.22-meter Lidar-derived DEM was resampled to 5-meter and 10-meter resolution while the 10-meter DEM was resampled to 5 and 1.22-meter resolutions. This was done to effectively perform statistical comparisons of the source DEM data and to create the 5-meter DEM datasets for the analyses; one resampled from the native 1.22-meter data and the other from the native 10-meter data.

Each of the two 5-meter DEMs produced through resampling was then processed to produce slope rasters for the area, in percent slope, and aspect rasters in values of degrees of rotation from north (0 to 360) and -1 for flat areas. The aspect values were further classified into the four cardinal (N, S, E, W) and four inter-cardinal (NW, NE, SW, SE) directions automatically during the generation process. This task was performed using the Slope and Aspect tools in Spatial Analyst.

The NLCD raster data were resampled to 5-meter resolution, clipped and then converted to vector data, using the Raster to Polygon tool, in order to easily combine some of the previously mentioned NLCD classification values to create a relevant dataset for analysis. The resulting seven values for the data (and their percentages of the ACC area) were: Barren Land (0.52%), Shrubland (0.7%), Herbaceous (15.58%), Forest (39.6%), Wetlands (3.64%), Developed (39.1%) and Open Water (0.87%). At this point, while the data were still in vector format, the area representing Developed land cover was exported and included in the vector data for processing. The full polygon NLCD data were then converted back to a 5-meter resolution raster with the Polygon to Raster tool for inclusion in the analyses. This is shown in Fig. 3-3.

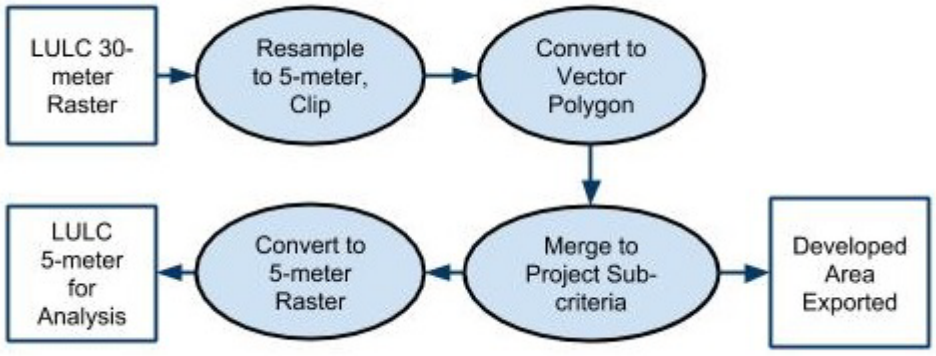

Fig. 3-3: LULC Processing

The vector data were used to create additional criteria layers for the analyses. The general process was to utilize the ArcGIS Buffer and Multi-ring Buffer tool to create polygon zones in accordance with the sub-criteria established. The polygonal vector data result was then converted to a 5-meter resolution raster with the Polygon to Raster tool and Clipped to the ACC boundary for inclusion in the primary analyses. The resulting data of the vector conversion of the criteria were the following 5-meter resolution rasters: ACC Developed Area Buffers, ACC Roads Buffers, ACC Land Use/Land Cover, ACC Electric Transmission Lines Buffers. This general process is shown in Fig. 3-4.

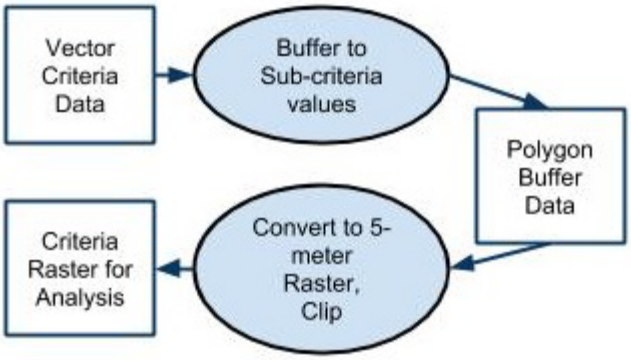

Fig. 3-4: Vector Criteria Data Processing

The raster criteria data generated from this analysis then were converted into Suitability Index Maps. This was accomplished by using the Reclassify tool to rank the criteria raster value ranges into integer values where 1 represented the most suitable sub-criteria, 2 the next most suitable and etc…. As an example, The ACC Roads raster was reclassified as shown in Fig. 3-5.

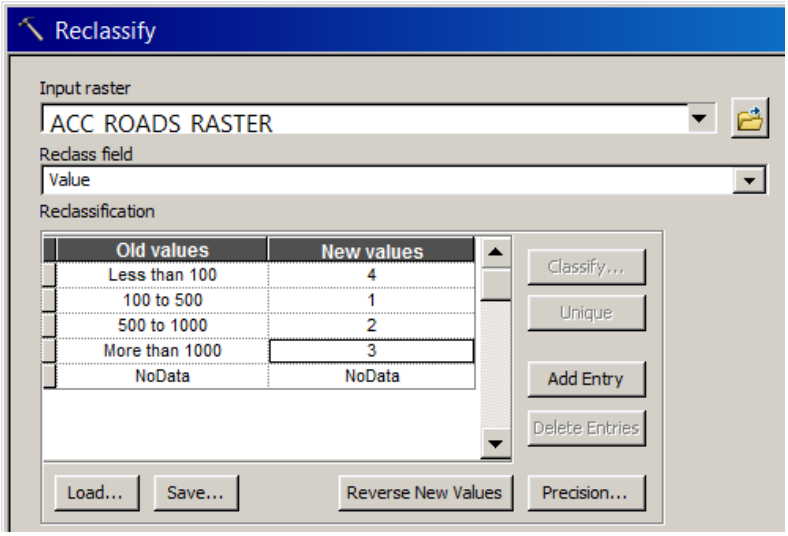

Fig. 3-5: Example of Reclassification of Criteria Suitability Index Raster

A Criteria Suitability Index Map was then generated for the constant spatial data in this project; Distance from Transmission Lines, Distance from Roads, Land Use/Land Cover and Distance from Developed Areas criteria, as shown in Fig. 3-6

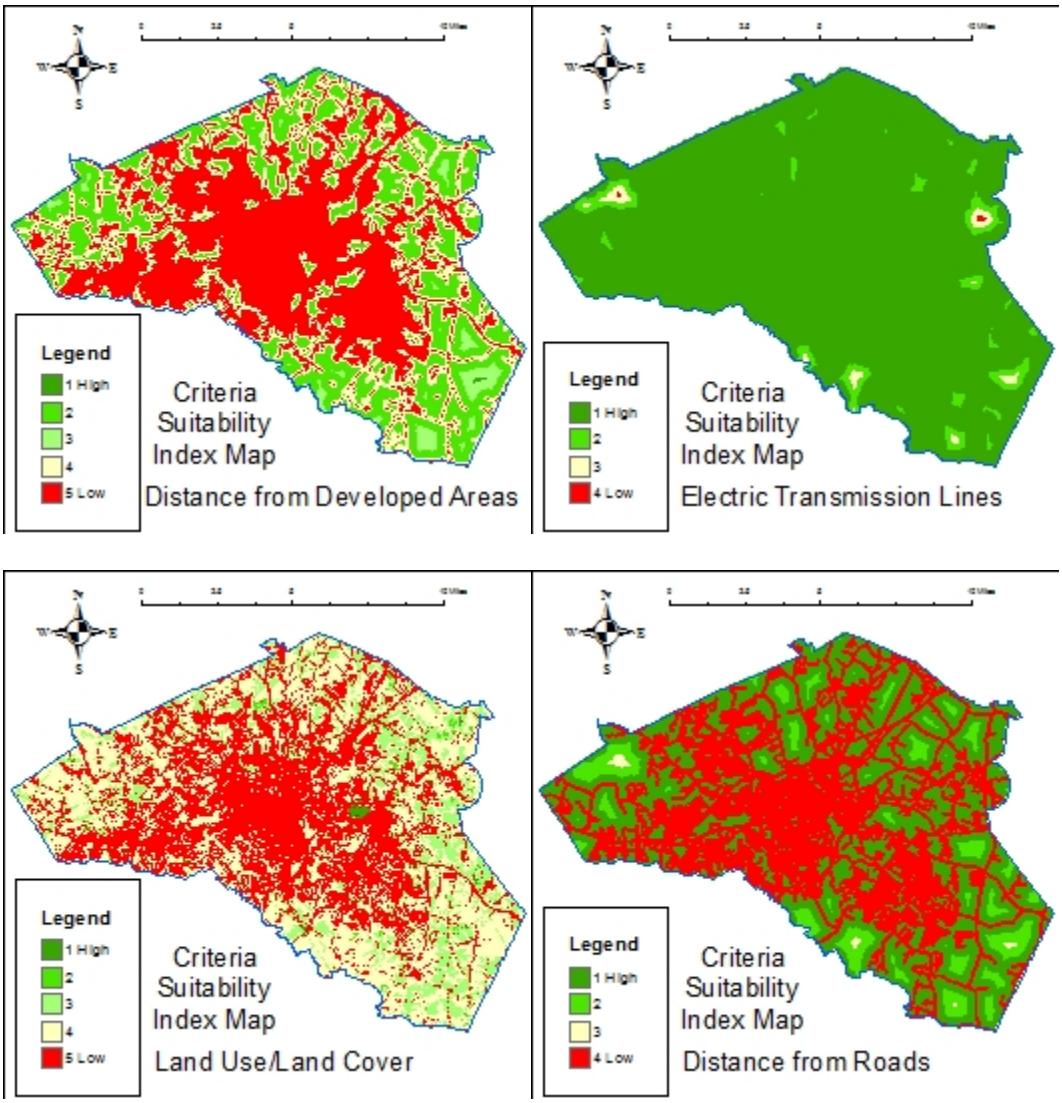

Fig. 3-6: Criteria Suitability Index Maps - Constants

For the slope and aspect criteria, a map was created for each source DEM original resolution that the 5m data was resampled from, as shown in Fig. 3-7:

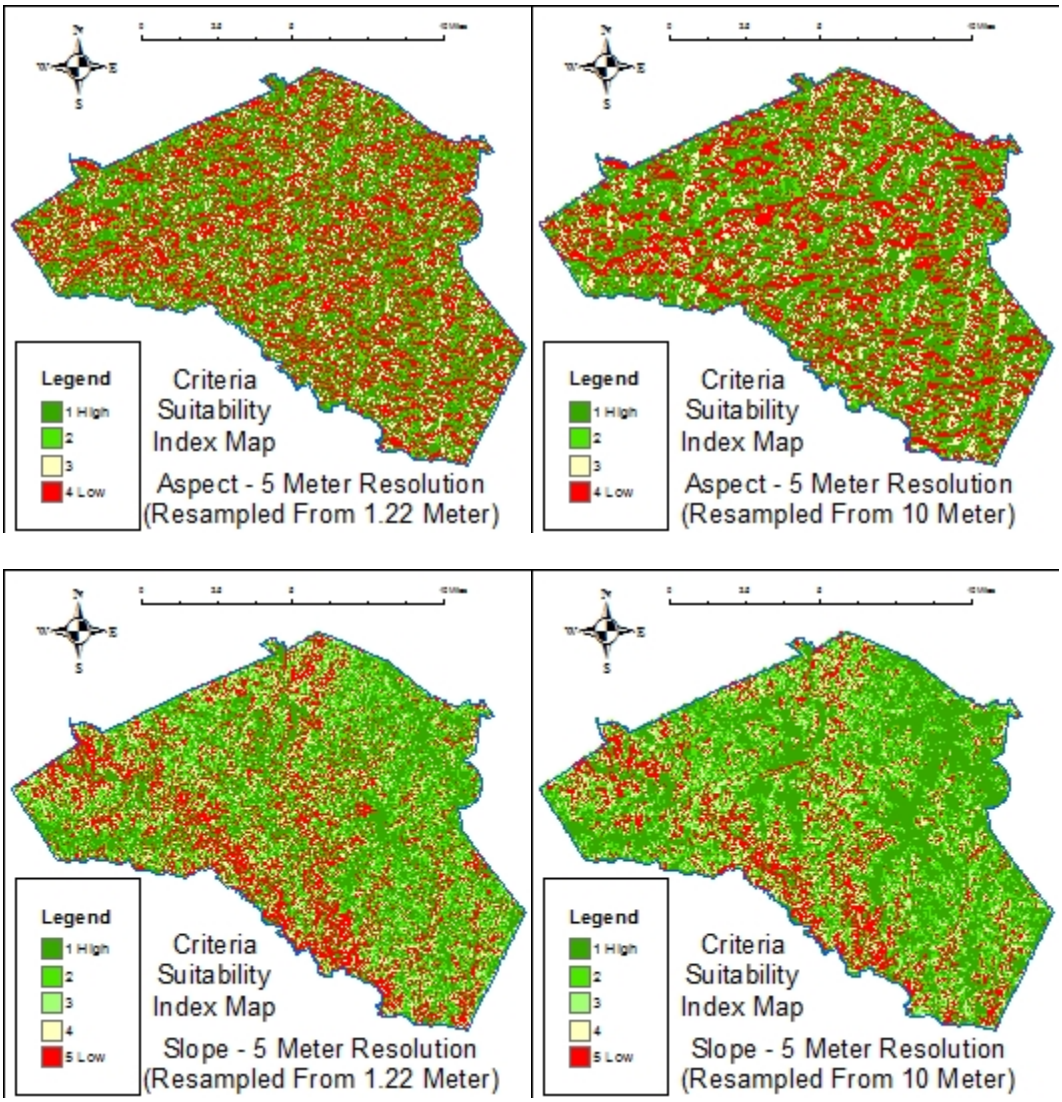

Fig. 3-7: Criteria Suitability Index Maps for Aspect and Slope

The Criteria Suitability Index Maps provide an opportunity for visual analysis of the suitability distribution across the project area and to see how the slope and aspect rasters are showing some deviation from each other.

The constraint data represents areas that are not suitable for SPVFs. These constraint areas were processed in a similar fashion to the vector criteria data. The constraints

typically were either a representation of a feature or a buffer around it so either direct export or the Buffer tool was utilized to accomplish their generation. This general process is depicted in Fig. 3-8.

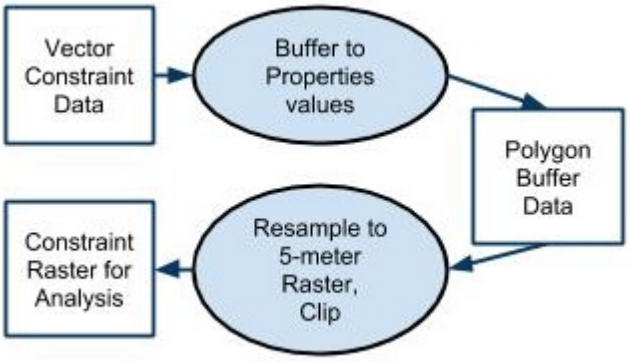

Fig. 3-8: Vector Constraint Processing

The resulting data of the vector conversion of the criteria were the following 5-meter resolution rasters: ACC Major Rivers/Streams Constraint, ACC All Rivers/Streams Constraint, ACC Lakes Constraint, ACC Wetlands Constraint, ACC Developed Areas Constraint. Their properties are summarized in Table 3-8:

Table 3-8: Properties of Constraint Layers

Constraint	Properties
ACC Major Rivers/Streams	150-meter buffer
ACC All Rivers/Streams	50-meter buffer
ACC Roads	100-meter buffer
ACC Lakes	Feature area and 50-meter buffer
ACC Wetlands	Feature area and 50-meter buffer
ACC Developed Areas	Feature area and 100-meter buffer

Once the individual constraint layers were created, they were merged into one constraint layer for ease of processing when utilized, as shown in Fig. 3-6:

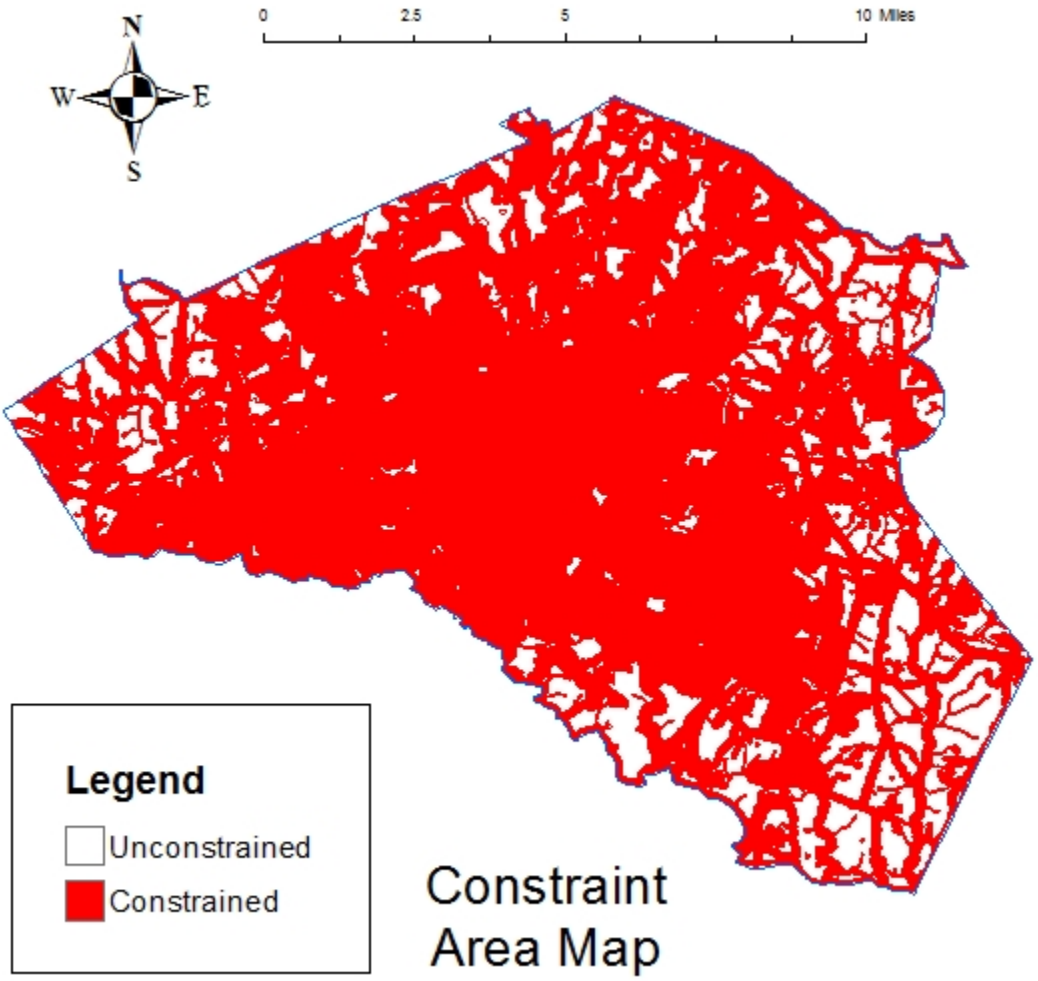

Fig. 3-6: Constraint Areas for Athens-Clarke County

One can readily see that there is a high degree of challenge in identifying suitable areas for SVPFs in ACC with 83.3% of the county constrained. That being the case, there is still an appreciable amount of area for consideration in the 17.7% remaining, which is 52.33 sq. km (20.20 sq. miles or 12,930 acres). The constraints were not applied to the

suitability model results, i.e., Land Suitability Map (LSM) until all other analysis was complete. The process of applying the constraints was to first reclassify the constraint raster as 0 for unconstrained and 99 for constrained and use the Raster Calculator tool to add that value to the LSM values of 1, 2, 3 or 4. The resulting raster could then be reclassified where the values of 1, 2, 3 and 4 would remain and 100, 101, 102 and 103 would be reassigned the value of 0. This would result in a final raster with the constrained areas "zeroed out" for suitability.

In order to find the top most suitable potential sites in ACC, the constrained LSM results from the 10-meter and 1.22-meter DEMs were selected for the top ten largest continuous areas with "Most" and "Good" suitability for an SPVF (Values 1 and 2) for Pass 1 and Pass 3. This was accomplished by converting each of the LSM rasters to polygons by using the Raster to Polygon tool. Those polygons were then sub-selected for suitability value 1 and 2 and those polygons exported, merged and exploded to create the individual continuous polygons. The areas of those polygons were sorted and the ten highest values were exported to a new data layer. Those final ten polygons from each of the LSM rasters processed represented the largest continuous regions of greater than or equal to "Good" suitability.

With the AHP developed and the data acquired and processed, the next step was to perform the overlay analyses to create the 5-m resolution rasters representing the Environmental Factors, the Economic Factors and then to overlay those to produce the LSM for each resolution tested.

Overlay Analysis

The overlay analyses were performed using Spatial Analyst Weighted Overlay tool for the creation of the Environmental Factors and Economic Factors rasters and the Weighted Sum tool for the combining of the Environmental and Economic Factors rasters into the Land Suitability Maps (LSM) for ACC. In order to create the data required to statistically compare the differences in models incorporating DEMs of different spatial resolutions, the processes were repeated with data from the 1.22-meter resolution DEM or the 10-meter DEM being the only variable in the process pairs. Fig. 3-7 shows the processes performed,

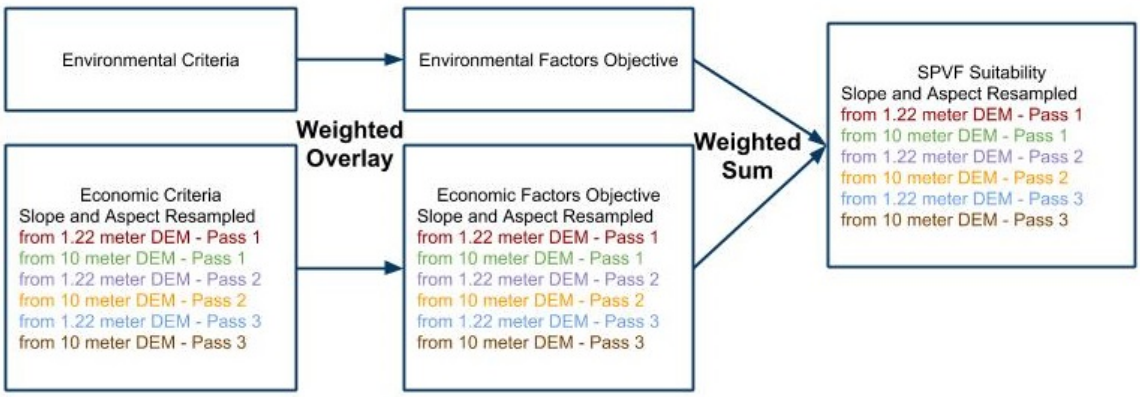

Fig. 3-7: Overlay Processes Performed

While achieving the same result is possible using the Raster Calculator tool, the Weighted Overlay tool in ArcGIS Spatial Analyst allows the organized combination of raster data modified by weights generated from MCDMs such as AHP. The Weighted Overlay tool interface allows one to adjust the evaluation scale in order to accommodate decimalized weights for the sub-criteria, as shown in Fig. 3-8:

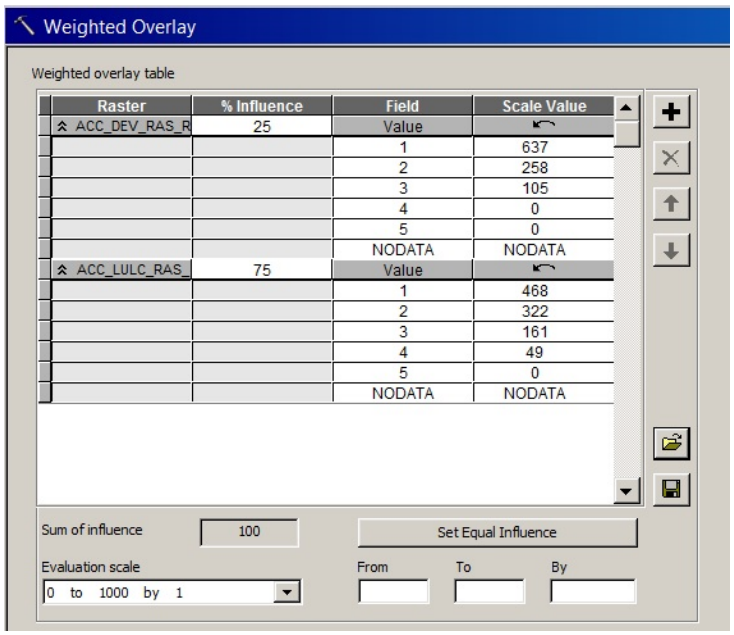

Fig. 3-8: Weighted Overlay Tool

It is important to note that the Weighted Overlay tool used in this manner produces a resulting raster with values having a larger range (due to the three orders of magnitude difference in the scale) but as long as both the Economic and Environmental rasters are created in the same manner, their values are scaled correctly relative to each other. Each of the Economic (one for each native resolution and pass) and Environmental raster data created was also resampled into four equal interval categories (low suitability, moderate suitability, good suitability and best suitability) for display purposes and will be shown and discussed in the results.

The Weighted Sum tool performs a similar and simpler operation by weighting the values of two or more rasters and summing them. This tool was used to combine the Environmental and Economic Objectives as shown in Fig. 3-9:

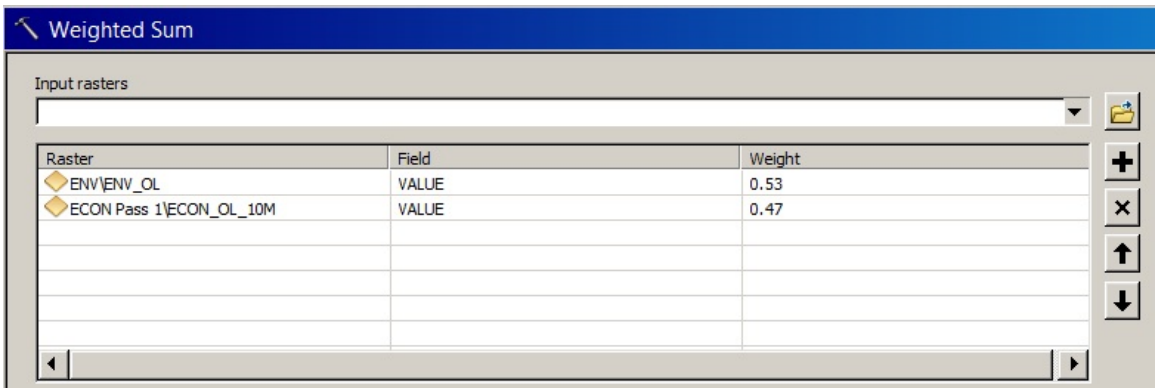

Fig. 3-9: Weighted Sum Tool

With the overlay analysis complete, the next step was to compare the data through statistical analysis. In order to perform appropriate statistical analyses, the constraint layer produced was not applied to the final LSM rasters until after that process was complete.

Statistical Analysis

The statistical approach of comparing the impact of the resolution data on soil mapping used by Shi et al. (2012) has been modified to test the correlation and deviation of the data generated in this study.

The first goal of the statistical analysis was to obtain the correlation coefficient, Normalized Root Mean Square Difference (NRMSD) and Coefficient of Variation of the RMSD (CV) of the DEM data in order to ascertain the similarity of the DEMs pre-processing. For some of the analyses, one cannot directly compare a 10-meter raster to a 1.22-meter raster and get meaningful results, so the method chosen was to “upsample”

the 10-meter DEM to 5-meter and 1.22-meter resolutions and “downsample” the 1.22-meter DEM to 5-meter and 10-meter resolutions, as discussed earlier.

The correlation coefficients of the DEM comparisons were calculated using Band Collection Statistics tool in ArcGIS Spatial Analyst with the ‘Compute covariance and correlation matrices’ option checked. The correlation of the data is how similarly the data change in relation to each other. This compared all of the six DEM data to each other as the process is not reliant on the resolution being matched for accuracy. This was repeated for the Economic Factors Objective and for the Land Suitability Map rasters, as well.

The NRMSD and CV were calculated in a more ‘manual’ process and were performed on the pairs at the same resolution (i.e., 10-meter NED DEM compared to 10-meter resolution from 1.22-meter “downsample”, 1.22-meter resolution from 10-meter “upsample” compared to 1.22-meter Lidar-derived DEM and 5-meter resolution from 1.22-meter “downsample” compared to 5-meter resolution from 10-meter “upsample”). The squared difference between the pairs of data were calculated using the Raster Calculator tool and inputting an equation (Equation 3-3).

Equation 3-3: Calculating Square Difference

$$\text{SQUARE}([\text{Raster 1}] - [\text{Raster 2}])$$

The order of Raster 1 and Raster 2 did not matter as the assumption was not made that any of the data were “the truth” and the goal was to measure the difference between the

pairs. The result was dubbed “Square Difference” for reference. General statistics (Count, Range, Mean, Standard Deviation, etc…) were then generated for the Square Difference rasters, as well as for the DEM input pairs, by using the Zonal Statistics as Table tool. This tool calculates standard raster statistics in a defined zone. In this case, that zone was defined by the border of ACC, so effectively the complete data area. The RMSD was calculated by taking the square root of the mean of the Square Difference raster and the NRMSD was calculated by dividing the RMSD by the Range of the DEM input pairs. The CV was calculated by dividing the RMSD by the Standard Deviation of the DEM input pairs. Because the Range and Mean values were different between the DEM input pairs, the lowest value was chosen to achieve the highest possible value for the comparison.

As the inputs for the overlay analysis derived from slope, the 5-meter aspect and slope rasters were compared. Aspect and slope data prove challenging in the nature of the data. Aspect values are -1 for flat surface and 0 to 360 depending on the angle of the aspect plane from north. When comparing the values of the two 5-meter aspect rasters, one must normalize the values to avoid having coincident rasters with values of 1 and 359 showing a difference of 358 when their true difference from each other is 2. This was accomplished but symbolizing the rasters aspect values as classified into 18 equal interval classes and then reclassifying the rasters values from 1 to 9 for 0 to 180 and 9 to 1 for 180 to 360. These are not suitability values, but just values for the purpose of statistical analysis. The result of this were that the aspect rasters had values from 1 to 9 where 1 represented northern aspect and 9 represented southern aspect and comparisons could be

made without using the original polar values. The slope was normalized as well, but classified by ¼ of the standard deviation of the 10-meter slope raster in 18 classifications in order to more successfully perform a data comparison of the densest set of values for percent slope for the region.

The statistical evaluation of slope and aspect was repeated using the reclassified data to see how the generalization of slope and aspect values into the suitability values affected the statistical analysis results.

Next, this process was repeated on the six Economic Objective rasters, one for each native resolution for each pass, created by the overlay process. The statistical analysis was performed on the "raw" output of the process rather than the reclassified data to retain more of the influence of the differences in the original data.

Finally, this process was repeated once again for the six Land Suitability Map rasters for each native resolution for each pass. These rasters were then subject to an additional analyses in the form of determining the absolute percentage difference between the percentages of the four suitability classifications for the project area.

At the conclusion of this project, it is the intent of the researcher to contact the ACC Planning Department and University of Georgia Campus Planning to inform them of the results of the study and to offer collaboration in developing an ACC SPVF Site Suitability Analysis customized to the criteria established by those entities.

CHAPTER 4

RESULTS & DISCUSSION

Unconstrained SPVF LSMs

Before discussing the statistical results of the study, it is helpful to see the Land Suitability Maps resulting from the process without the constraints applied to visually compare them. As mentioned in the methods, in order to test the influence of the weight of aspect and slope on the AHP process, three Passes were performed for each source resolution, (i.e., Pass 1-10-meter and Pass 1-1.22-meter, Pass 2-10-meter and Pass 2-1.22-meter, and Pass 3-10-meter and Pass 3-1.22-meter). The two maps in which the weights of the aspect and slope are at their lowest, are shown in in Fig. 4-1 and 4-2:

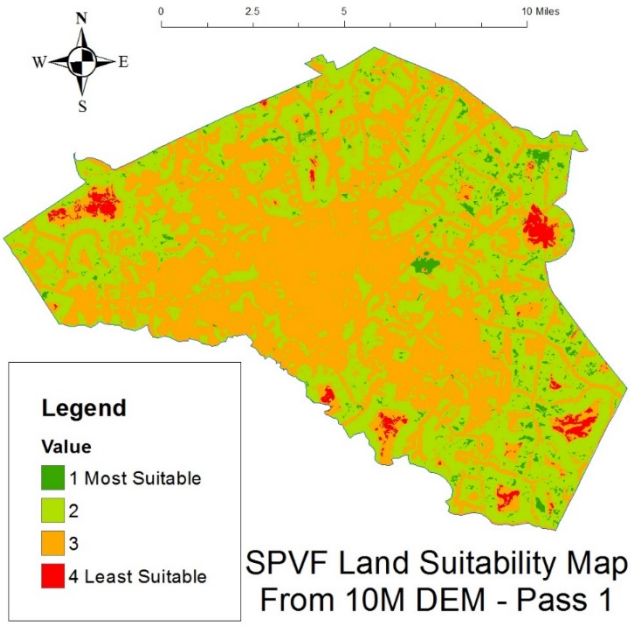

Fig. 4-1: LSM – Pass 1 – From 10-meter DEM Data – Unconstrained

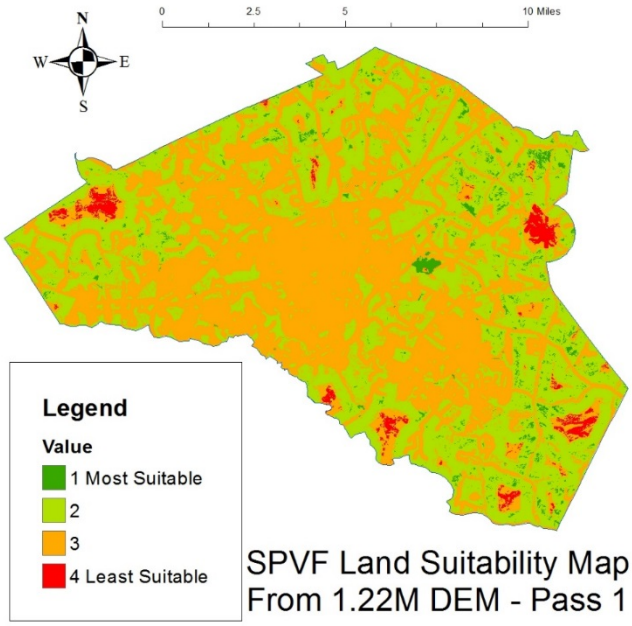

Fig. 4-2: LSM – Pass 1 – From 1.22-meter DEM Data – Unconstrained

Pass 2 represents an increase in the weights of both aspect and slope relative to the Distance from Transmission Lines and Distance from Roads data input into analysis, as shown in Fig. 4-3 and Fig. 4-4:

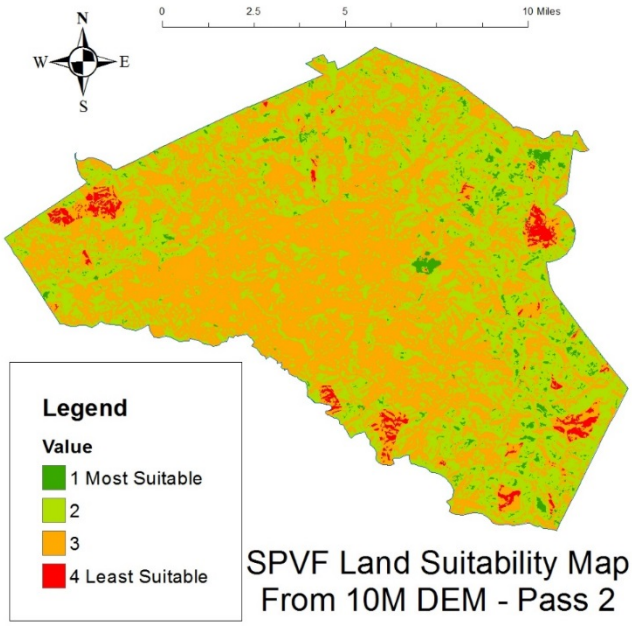

Fig. 4-3: LSM – Pass 2 – From 10-meter DEM Data – Unconstrained

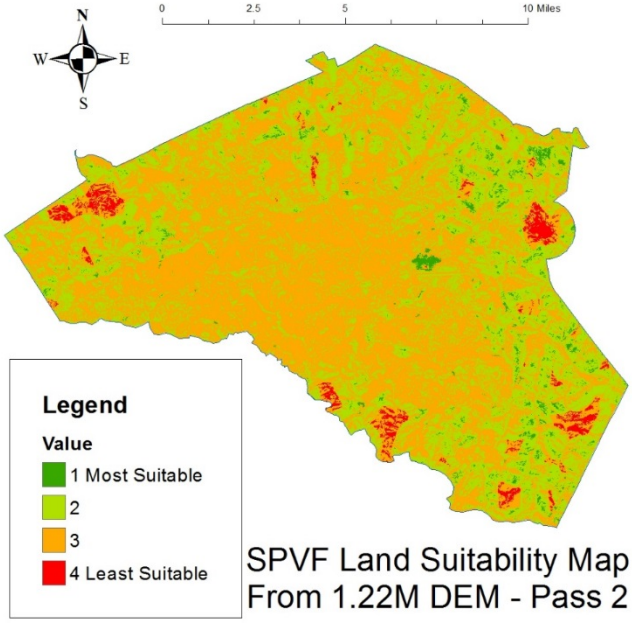

Fig. 4-4: LSM – Pass 2 – From 1.22-meter DEM Data – Unconstrained

In Pass 3 the weights of both aspect and slope relative to the Distance from Transmission Lines and Distance from Roads data are at their highest, as shown in Fig. 4-5 and Fig. 4-6:

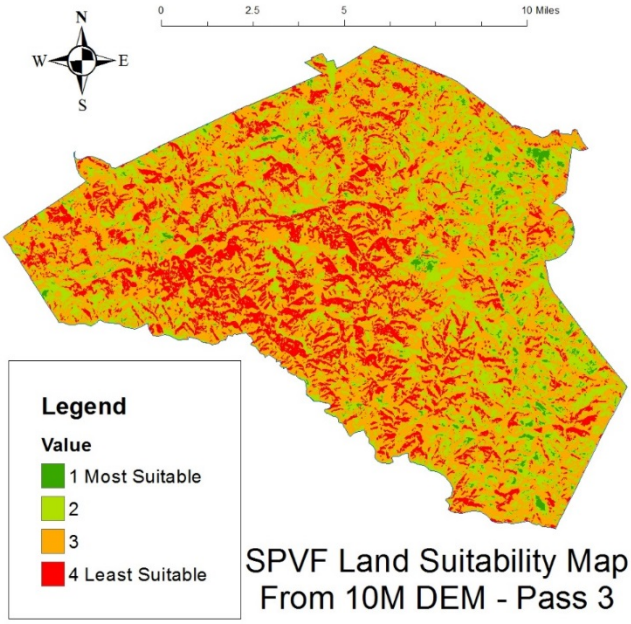

Fig. 4-5: LSM – Pass 3 – From 10-meter DEM Data – Unconstrained

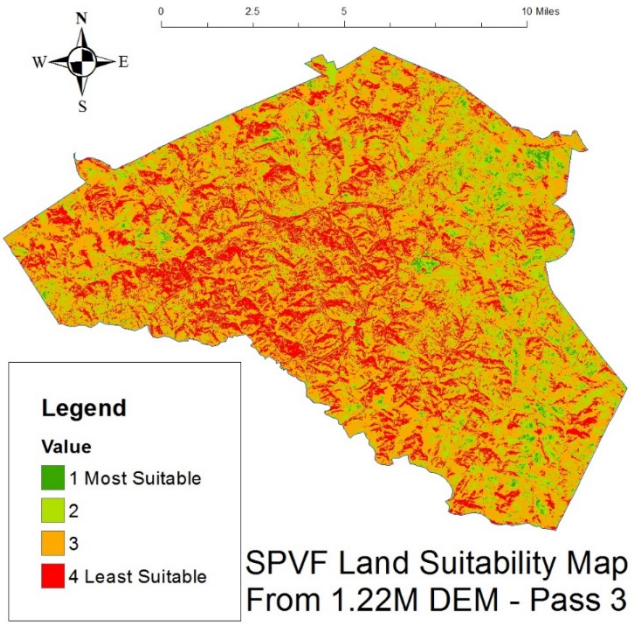

Fig. 4-6: LSM – Pass 3 – From 1.22-meter DEM Data – Unconstrained

The differences, or lack thereof, both within and between the passes are visually apparent as the slope and aspect increase in weight. Having just viewed the resulting Land Suitability Maps for SVPFs in ACC from the 10-meter and 1.22-meter native resolutions and at the differing weights of the three passes, a discussion of the visual analysis is in order.

At the level of Pass 1, it is visually difficult to tell a difference between the 10-meter and 1.22-meter resolution derived products, shown in Fig. 4-7:

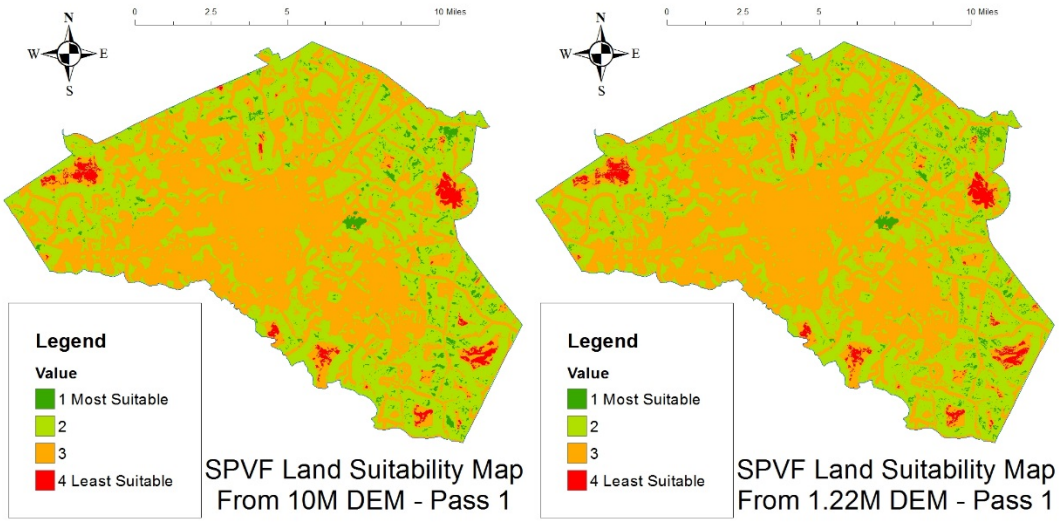

Fig. 4-7: Visual Comparison of LSM - Pass 1 - Unconstrained

At the level of Pass 2, it is still difficult to tell a visual difference between the 10-meter and 1.22-meter resolution derived products with the increase in weights of our variables of aspect and slope from 10% total influence on the suitability to 20%, though the noisiness of the data seems to be increasing with that change, as shown in Fig. 4-8:

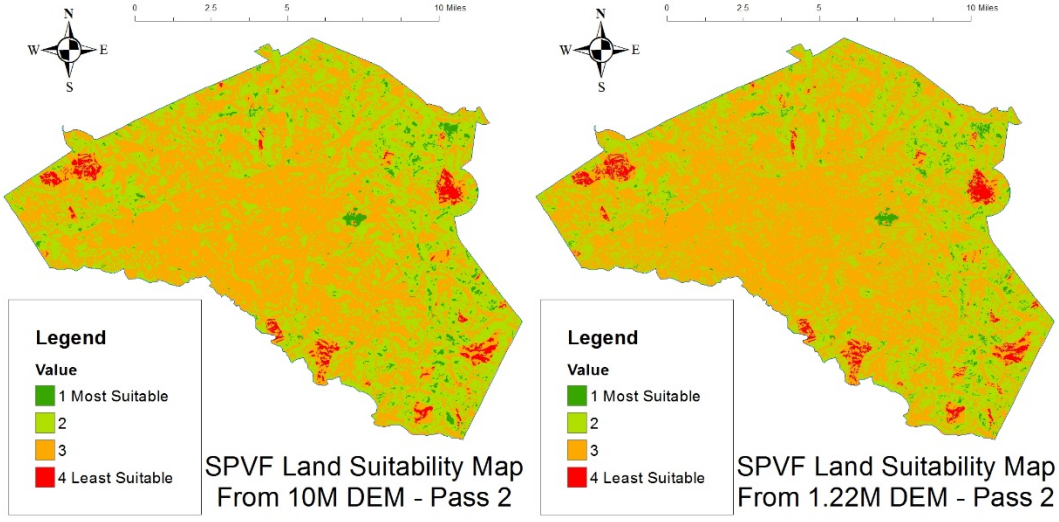

Fig. 4-8: Visual Comparison of LSM – Pass 2 - Unconstrained

At the level of Pass 3, however, with aspect and slope constituting a total of 72% of the weight of the Economic Factors Objective and roughly 36% of the total model, one can readily observe a difference between the 10-meter and 1.22-meter resolution derived products. The areas of suitability are denser in the 10-meter product with a more noisy appearance to the 1.22-meter product, as shown in Fig. 4-9:

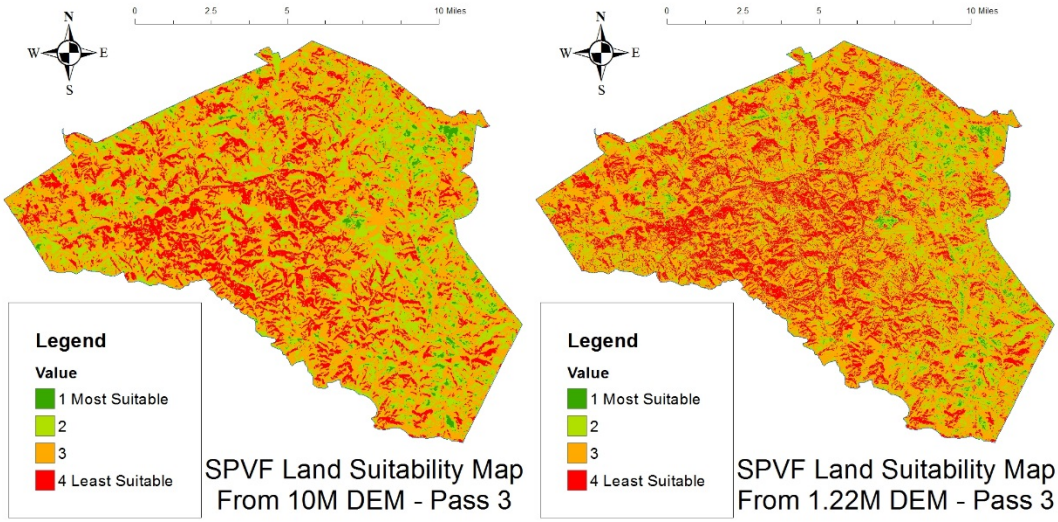

Fig. 4-9: Visual Comparison of LSM - Pass 3 - Unconstrained

Statistical Analysis Results

As previously mentioned, an important statistic for DEM data is the correlation coefficient, or correlation, which conveys whether the data being compared change in a similar fashion. The closer the correlation, the more similar the changes in the data.

The correlation of the DEM data, as shown, in Table 4-1, shows that the correlation between all of the DEMs and their resampling was very high.

Table 4-1: DEM Correlation Matrix

	DEM 10M	**DEM 5M (From 10M)**	**DEM 1.22M (From 10M)**	**DEM 10M (From 1.22M)**	**DEM 5M (From 1.22M)**	**DEM 1.22M**
DEM 10M	1.0000	0.9989	0.9975	0.9868	0.9866	0.9744
DEM 5M (From 10M)	0.9989	1.0000	0.9985	0.9867	0.9872	0.9752
DEM 1.22M (From 10M)	0.9975	0.9985	1.0000	0.9855	0.9859	0.9760
DEM 10M (From 1.22M)	0.9868	0.9867	0.9855	1.0000	0.9982	0.9832
DEM 5M (From 1.22M)	0.9866	0.9872	0.9859	0.9982	1.0000	0.9836
DEM 1.22M	0.9744	0.9752	0.9760	0.9832	0.9836	1.0000
Average Correlation		**0.9891**				

The average correlation of 0.9891 reinforces that claim of similarity among all of the DEM data. When one looks specifically at the correlation of the two 5-meter resamples from the 1.22-meter and 10-meter source data being 0.9872, the claim can be made that the data utilized for comparison in this study were statistically similar as regards to how the data varied over the survey area. Next, the RMSD was examined for the DEM data. As shown in Table 4-2, The RMSD, normalized RMSD and CV were low and consistent for the data being compared.

Table 4-2: DEM Statistics and Deviation

Layer	Range	Mean	Standard Dev.	RMSD	NRMSD	CV
DEM 1.22M	478.226	699.436	61.720			
DEM 1.22M (From 10M)	351.448	700.408	61.438			
Square Difference	154616.000	80.134	2017.471	8.952	1.9%	1.3%
DEM 10M	351.565	700.374	61.480			
DEM 10M (From 1.22M)	476.733	699.433	61.720			
Square Difference	154245.400	95.012	2363.115	9.747	2.8%	1.4%
DEM 5M (From 1.22M)	477.470	699.434	61.720			
DEM 5M (From 10M)	351.313	700.420	61.437			
Square Difference	154055.700	94.140	2354.910	9.703	2.8%	1.4%

The values indicate a low residual variance between the data and the resolution pairs indicated. This validates the use of the resampling technique to create resolution-matched 5-meter data from the 10-meter and 1.22-meter source data for the purpose of performing the analysis in this study.

The statistical analysis of the 5-m aspect and slope rasters show a much different result. The correlation and deviation of the data was nowhere near the level of the DEMs they were derived from. Table 4-3 summarizes this result.

Table 4-3: Aspect and Slope Statistics – Reclassed to Integer

Layer	Range	Mean	Standard Dev.	RMSD	NRMSD	COV
Aspect 5M (1.22M) Reclassed	8.000	5.226	2.577			
Aspect 5M (10M) Reclassed	8.000	5.278	2.534			
Square Difference	64.000	4.461	8.904	2.112	26.4%	40.0%
Slope 5M (1.22M) Reclassed	17.000	6.972	4.370			
Slope 5M (10M) Reclassed	17.000	6.038	3.727			
Square Difference	289.000	15.442	33.029	3.930	23.1%	65.1%
Aspect Correlation	0.659					
Slope Correlation	0.565					

This lower level of correlation and higher error seems to present the potential for introducing difference between the paired results at each pass increasing as the influence of slope and aspect increase. To truly test this, the statistics on the slope and aspect suitability rasters actually input into the overlay analysis were generated. The results are presented in Table 4-4:

Table 4-4: Aspect and Slope Statistics – Reclassed to Suitability

Layer	Range	Mean	Standard Dev.	RMSD	NRMSD	COV
Aspect 5M (1.22M) Suitability	3.000	2.385	1.320			
Aspect 5M (10M) Suitability	3.000	2.359	1.304			
Square Difference	9.000	1.321	2.486	1.149	38.3%	48.7%
Slope 5M (1.22M) Suitability	4.000	2.634	1.592			
Slope 5M (10M) Suitability	4.000	2.319	1.485			
Square Difference	16.000	2.319	4.010	1.523	38.1%	65.7%
Aspect Correlation	0.616					
Slope Correlation	0.533					

The results from this analysis show little difference form the other approach to compare the slope and aspect values. It appears that slope and aspect will be a source deviation in the model and will increase with the increase of the weight of the slope and aspect criteria with the passes. The next statistical comparison performed was after the Economic Objective rasters were generated with the weighted overlay analyses. In Table 4-5, we can see that the story of the correlation of the data changes somewhat.

Table 4-5: Economic Objective Correlation Matrix

	ECON 5M (1.22M) - Pass 1	**ECON 5M (10M) - Pass 1**	**ECON 5M (1.22M) - Pass 2**	**ECON 5M (10M) - Pass 2**	**ECON 5M (1.22M) - Pass 3**	**ECON 5M (10M) - Pass 3**
ECON 5M (1.22M) - Pass 1	1.0000	0.9461	0.7898	0.6709	0.5565	0.4076
ECON 5M (10M) - Pass 1	0.9461	1.0000	0.6720	0.7890	0.4083	0.5561
ECON 5M (1.22M) - Pass 2	0.7898	0.6720	1.0000	0.7419	0.8899	0.5658
ECON 5M (10M) - Pass 2	0.6709	0.7890	0.7419	1.0000	0.5645	0.8901
ECON 5M (1.22M) - Pass 3	0.5565	0.4083	0.8899	0.5645	1.0000	0.5913
ECON 5M (10M) - Pass 3	0.4076	0.5561	0.5658	0.8901	0.5913	1.0000
Average Correlation		**0.7244**				

When comparing the correlation at Pass 1, we see a correlation near the level of the DEM data. At Pass 2 and Pass 3, with the weights of the DEM-derived data (aspect and slope) increasing, the correlation drops dramatically between the 10-meter and 1.22-meter derived data pairs. An interesting result is the fairly high correlation maintained, and even increasing, when comparing the same source resolution across adjacent passes (i.e., Econ 5-M from 10-M Pass 1 to Econ 5-M from 10-M Pass 2, Econ 5-M from 10-M Pass 2 to Econ 5-M from 10-M Pass 3, etc…), highlighted in dark gray.

When looking at the deviation and variation of the Economic Objective data, a similar result is observed. In Table 4-6, the NRMSD and CV increase as the weights increase in each pass.

Table 4-6: Economic Objective Statistics and Deviation

	Range	**Mean**	**Standard Dev.**	**RMSD**	**NRMSD**	**CV**
ECON 5M(1.22M) - Pass 1	611.000	481.385	103.207			
ECON 5M(10M) - Pass 1	594.000	485.975	103.099			
Square Difference	15376.000	1167.282	1935.394	34.166	5.8%	7.0%
ECON 5M(1.22M) - Pass 2	600.000	471.770	94.424			
ECON 5M(10M) - Pass 2	592.000	480.934	94.475			
Square Difference	53824.000	4688.431	7771.847	68.472	11.6%	14.2%
ECON 5M(1.22M) - Pass 3	590.000	364.058	135.123			
ECON 5M(10M) - Pass 3	582.000	380.576	135.091			
Square Difference	173889.000	15193.160	25181.990	123.261	21.2%	32.4%

This result is an expression of the differences observed in the slope and aspect data. As the influence of the slope and aspect on the Economic Objective is 20% at Pass 1, 40% at Pass2 and 72% on Pass 3, this is not an unexpected result. The reintroduction of the Environmental Objective in attaining the AHP model will mitigate this effect.

Finally, statistical analyses were performed on the LSM rasters. With the introduction of the Environmental Objective, the impact introduced by the weight increase of aspect and slope in the three passes is reduced. The correlation in the data is improved, as shown in Table 4-7:

Table 4-7: LSM Correlation Matrix

	LSM 5M (1.22M) - Pass 1	**LSM 5M (10M) - Pass 1**	**LSM 5M (1.22M) - Pass 2**	**LSM 5M (10M) - Pass 2**	**LSM 5M (1.22M) - Pass 3**	**LSM 5M (10M) - Pass 3**
LSM 5M (1.22M) - Pass 1	1	0.97113	0.88945	0.82191	0.703	0.61094
LSM 5M (10M) - Pass 1	0.97113	1	0.82299	0.88927	0.60999	0.70455
LSM 5M (1.22M) - Pass 2	0.88945	0.82299	1	0.84463	0.91544	0.70063
LSM 5M (10M) - Pass 2	0.82191	0.88927	0.84463	1	0.69781	0.91651
LSM 5M (1.22M) - Pass 3	0.703	0.60999	0.91544	0.69781	1	0.69755
LSM 5M (10M) - Pass 3	0.61094	0.70455	0.70063	0.91651	0.69755	1
Average Correlation		**0.8220**				

The deviation statistics show a similar effect similar for the LSM rasters, as shown in Table 4-8:

Table 4-8: LSM Statistics and Deviation

	Range	Mean	Standard Dev.	RMSD	NRMSD	CV
LSM 5M(1.22M) - Pass 1	507.650	255.102	66.316			
LSM 5M(10M) - Pass 1	499.660	257.258	66.366			
Square Difference	3396.559	257.853	427.529	16.039	3.2%	6.2%
LSM 5M(1.22M) - Pass 2	502.480	250.583	57.120			
LSM 5M(10M) - Pass 2	491.200	254.888	57.331			
Square Difference	11889.720	1035.675	1716.801	15.965	3.3%	6.3%
LSM 5M(1.22M) - Pass 3	497.780	199.958	73.696			
LSM 5M(10M) - Pass 3	493.550	207.720	73.951			
Square Difference	38412.090	3356.169	5562.701	57.932	11.7%	27.9%

Another statistical analysis performed for the LSM rasters was determining the absolute percentage difference between the percentages of the four suitability classifications for the project area. The results for Pass 1, Pass 2 and Pass 3 are shown in Table 4-9, 4-10 and 4-11:

Table 4-9: Absolute % Difference of Suitability Area (Sq. km) - Pass 1

	LSM Area 5M(1.22M) - Pass 1	LSM Area 5M(10M) - Pass 1	LSM % 5M(1.22M) - Pass 1	LSM % 5M(10M) - Pass 1	Absolute Difference
Best Suitability	6.24	7.25	1.99%	2.31%	0.32%
Good Suitability	141.43	142.05	45.03%	45.23%	0.21%
Moderate Suitability	160.93	159.46	51.24%	50.78%	0.46%
Low Suitability	5.49	5.27	1.75%	1.68%	0.07%

Table 4-10: Absolute % Difference of Suitability Area (Sq. km) - Pass 2

	LSM Area 5M(1.22M) - Pass 2	LSM Area 5M(10M) - Pass 2	LSM % 5M(1.22M) - Pass 2	LSM % 5M(10M) - Pass 2	Absolute Difference
Best Suitability	5.73	6.85	1.82%	2.18%	0.36%
Good Suitability	124.98	135.19	39.79%	43.05%	3.26%
Moderate Suitability	177.26	166.37	56.44%	52.98%	3.46%
Low Suitability	6.12	5.64	1.95%	1.79%	0.15%

Table 4-11: Absolute % Difference of Suitability Area (Sq. km) - Pass 3

	LSM Area 5M(1.22M) - Pass 3	LSM Area 5M(10M) - Pass 3	LSM % 5M(1.22M) - Pass 3	LSM % 5M(10M) - Pass 3	Absolute Difference
Best Suitability	4.52	5.74	1.44%	1.83%	0.39%
Good Suitability	70.01	80.88	22.29%	25.76%	3.47%
Moderate Suitability	167.83	164.99	53.43%	52.54%	0.89%
Low Suitability	71.74	62.42	22.84%	19.88%	2.96%

Constrained SPVF LSMs

The constraints were applied to the six LSM rasters. These final products represent the available area of low to high suitability in ACC for SPVFs.

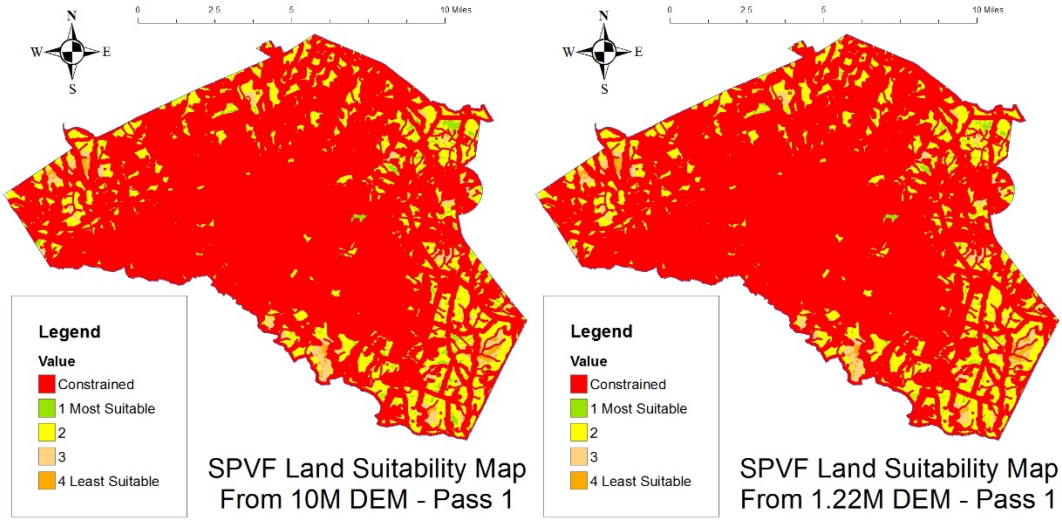

Fig. 4-10: Visual Comparison of LSM – Pass 1 - Constrained

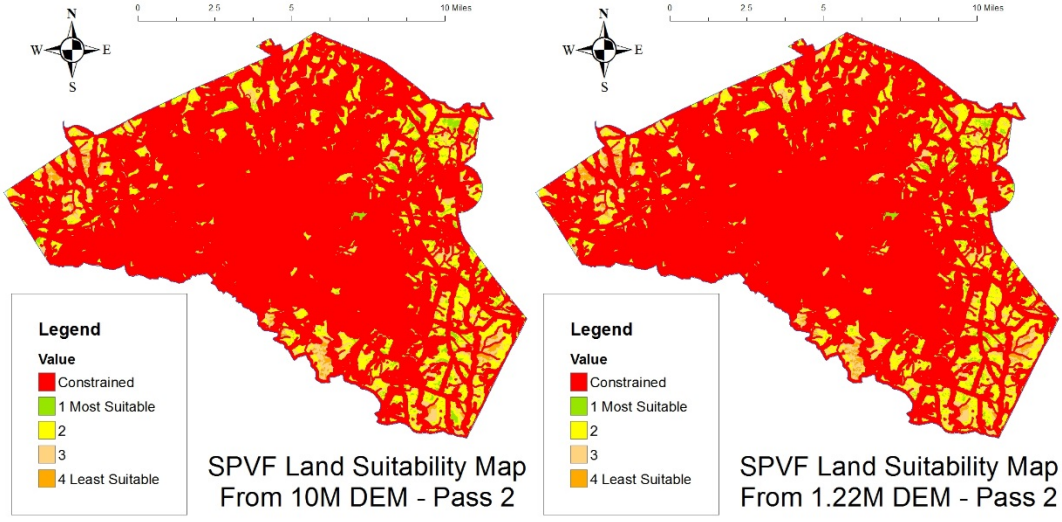

Fig. 4-11: Visual Comparison of LSM – Pass 2 - Constrained

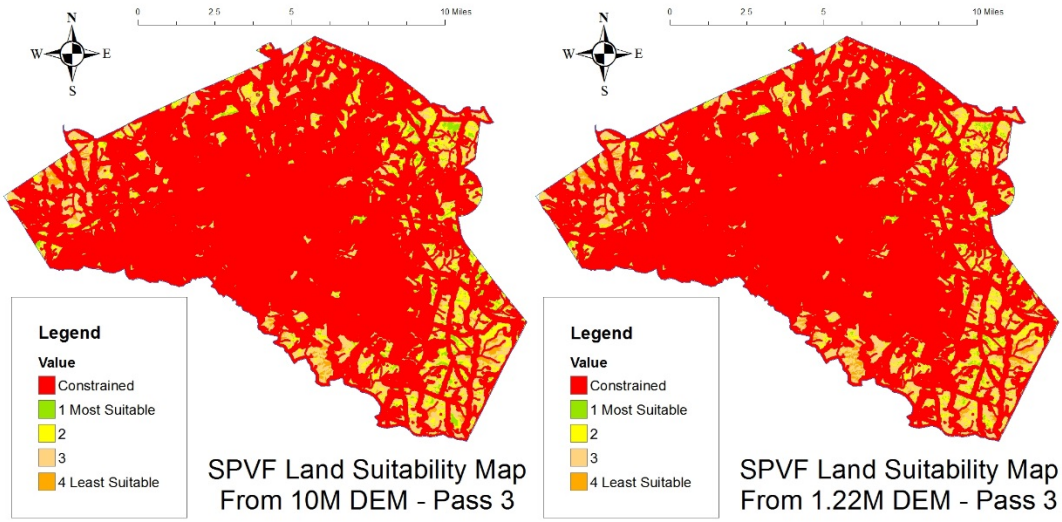

Fig. 4-12: Visual Comparison of LSM – Pass 3 - Constrained

There is a high degree of visual similarity between these maps. The high suitability areas are consistent, if not exactly the same in size or continuity. That is not saying the results are identical, but if one were to visually analyze the extremes of each of these maps, these same three example areas of “Most Suitable” would stand out. By performing a visual assessment, such areas of high concentration of “Most Suitable”, common to the 10-meter and 1.22-meter LSMs can be selected as shown in in Fig. 4-13 and Fig. 4-14.

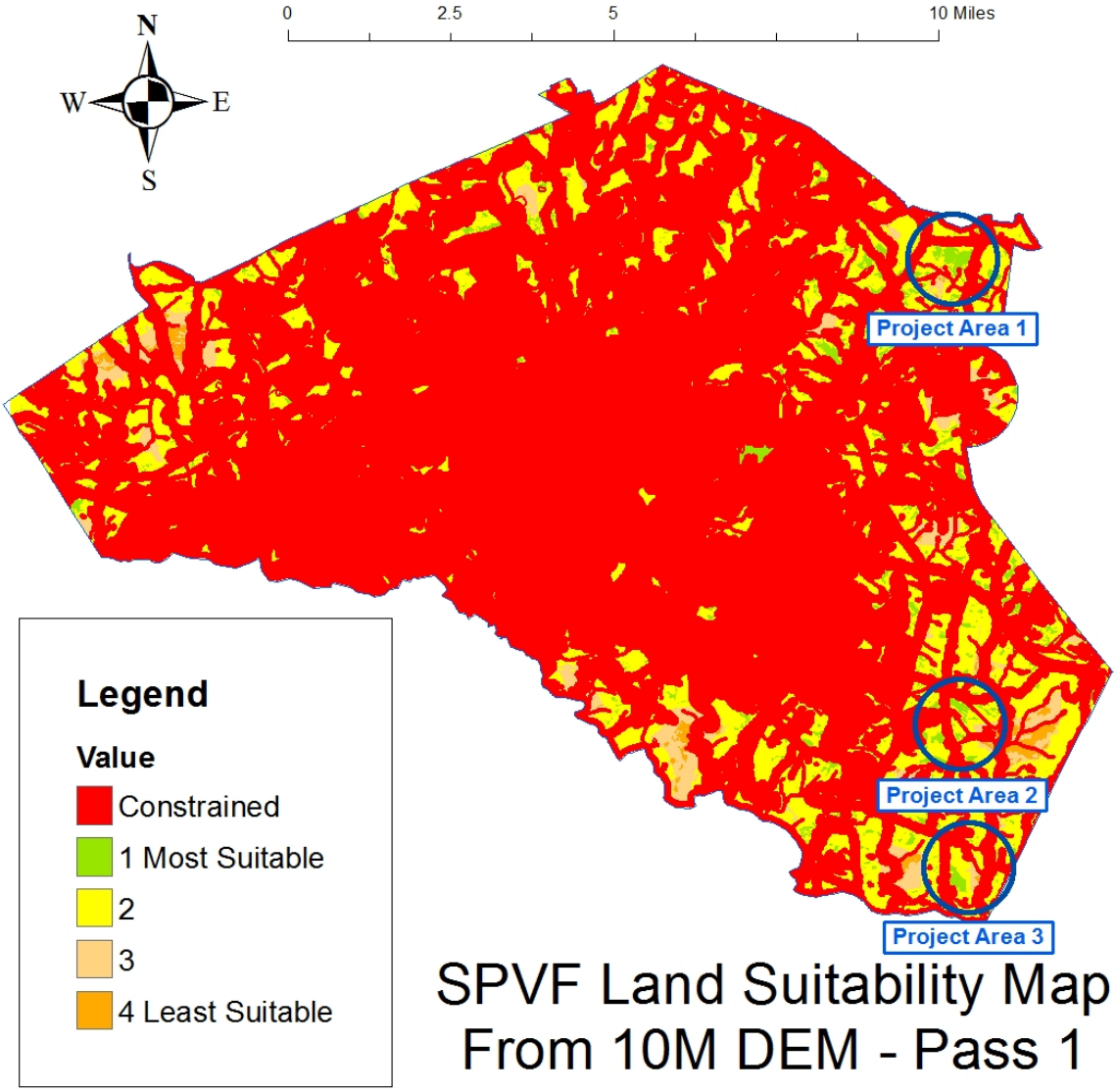

Fig. 4-13: Suitable Area Project Overview Map - From 10-M Res. - Pass 1

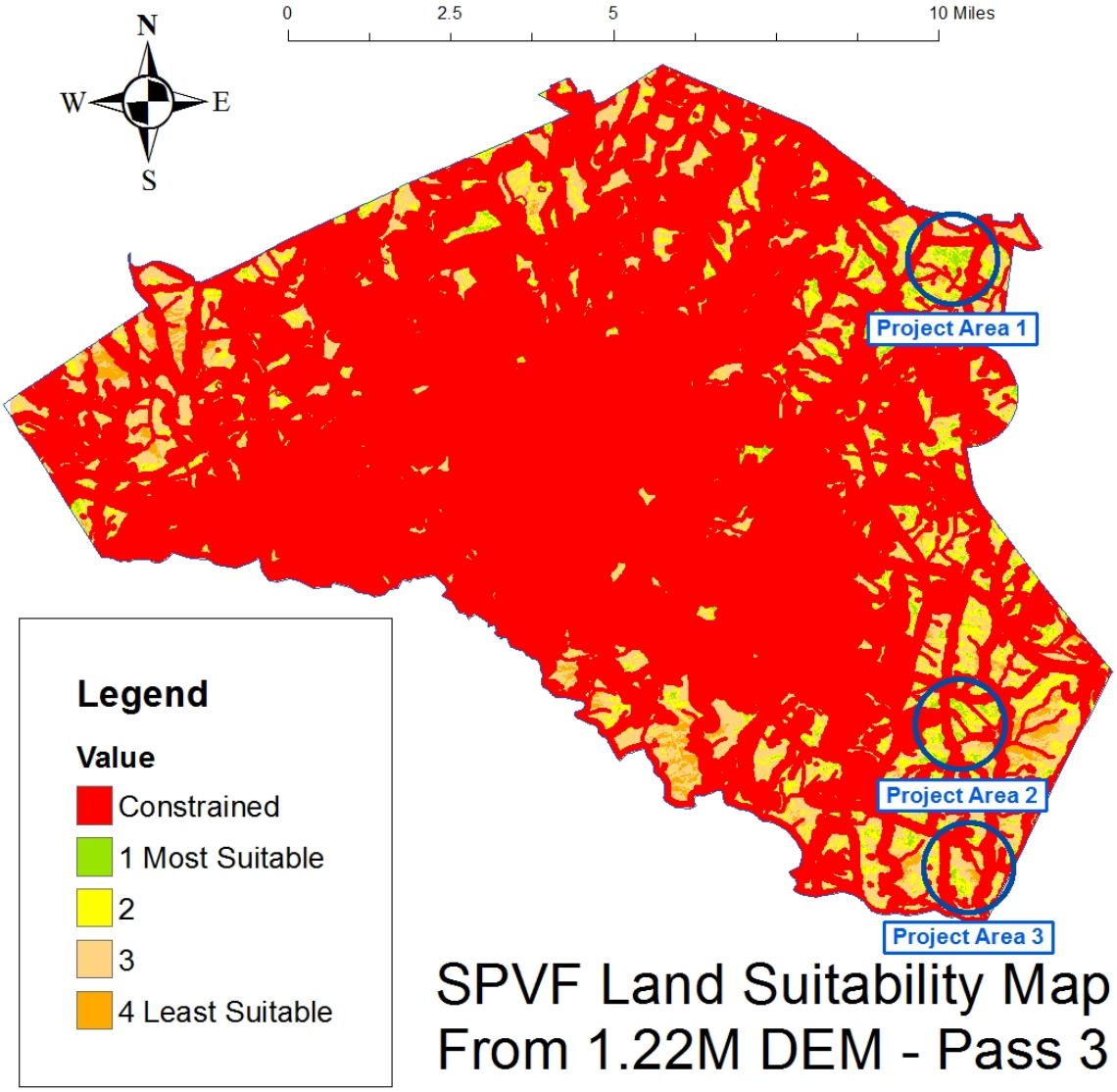

Fig. 4-14: Suitable Area Project Overview Map - From 1.22-M Res. - Pass 3

Project Areas

With these three project areas visually apparent from the SVPF LSMs, we can take a closer look at the areas to see what kind of solar output could be realized from SVPFs located there. The current industry estimate for SVPFs capacity (the amount of power that can be produced at a given point in time) is 1 Megawatt (MW) for every 2.02

Hectares (5 Acres) of SVPF. Then, the Capacity Factor, which is the percentage of the capacity that is typically realized over time, must be considered. For SVPFs, this is 20%. To determine how much power that an SVPF actually produces over a year (8,760 hours), the following formula (Equation 4-1) can be used:

Equation 4-1: Solar Farm Electrical Production Formula

$$\text{Capacity (MW)} * 8{,}760 \text{ hours/year} * \text{Capacity Factor} = \text{MWh/yr}$$

In 2013, the average annual electricity consumption for a Georgia residential utility customer was 13.056 Megawatt-hours/year (MWh/yr). In 2013, each MWh sold at an average of $114.6 /MWh. This information was used to determine how many average homes could be powered by SVPFs fully utilizing each Project Area and how much money that electricity produced represented in 2013

Project Area One is an example of a potential site that is large and continuous (Fig. 4-15).

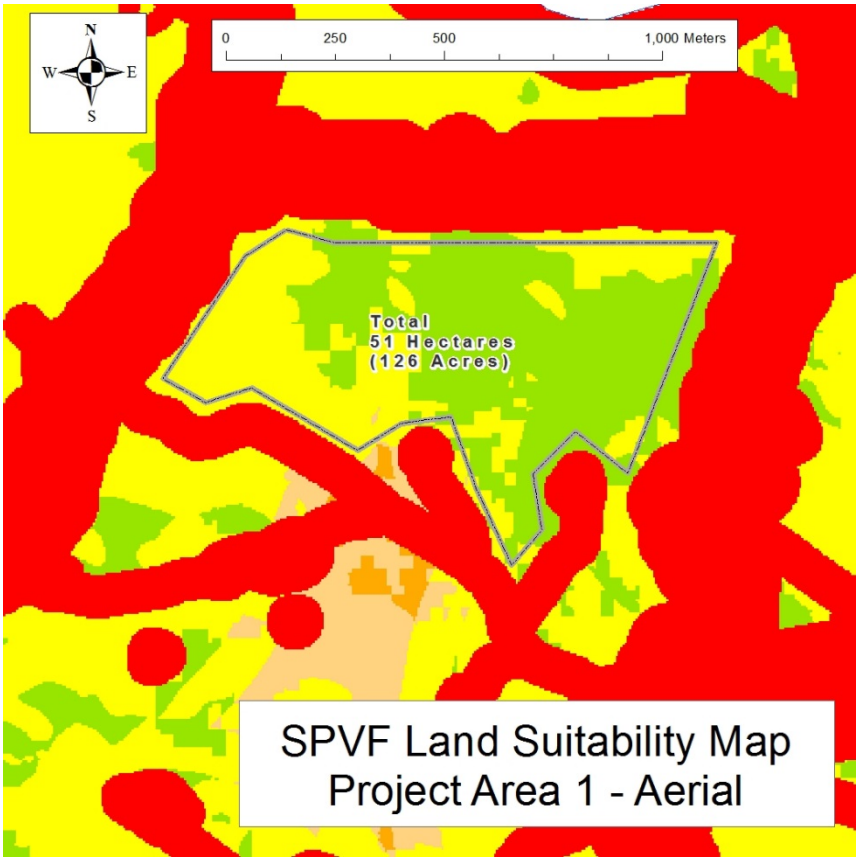

Fig. 4-15: Suitability of Project Area One

In this area, 51 Hectares (126 Acres) are identified as largely Best Suitability for a SVPF. Visual analysis of the aerial photography (Fig. 4-16) shows a reasonable agreement between ground conditions and the suitability indicated by the model.

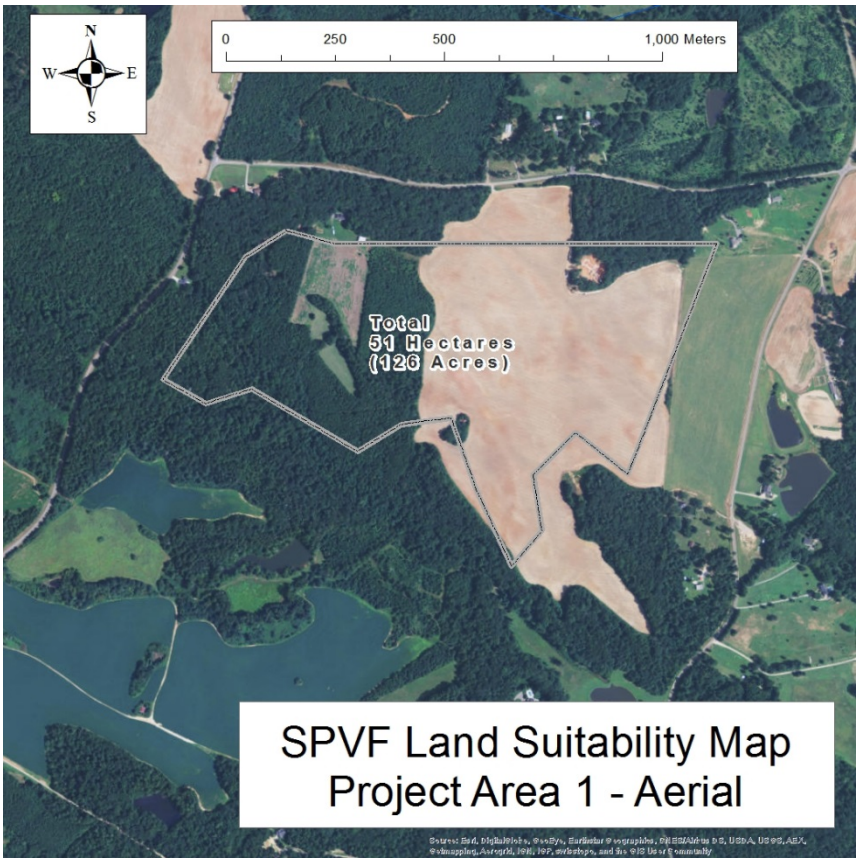

Fig. 4-16: Aerial of Project Area One

Project Area Two is an example of a potential site that is discontinuous. While these suitable areas are separated by constrained areas (as shown in Fig. 4-17), the proximity of the three sites to each other could facilitate maintenance of the site. In this area, 47.75 Hectares (118 Acres) are identified as largely Best Suitability for a SVPF.

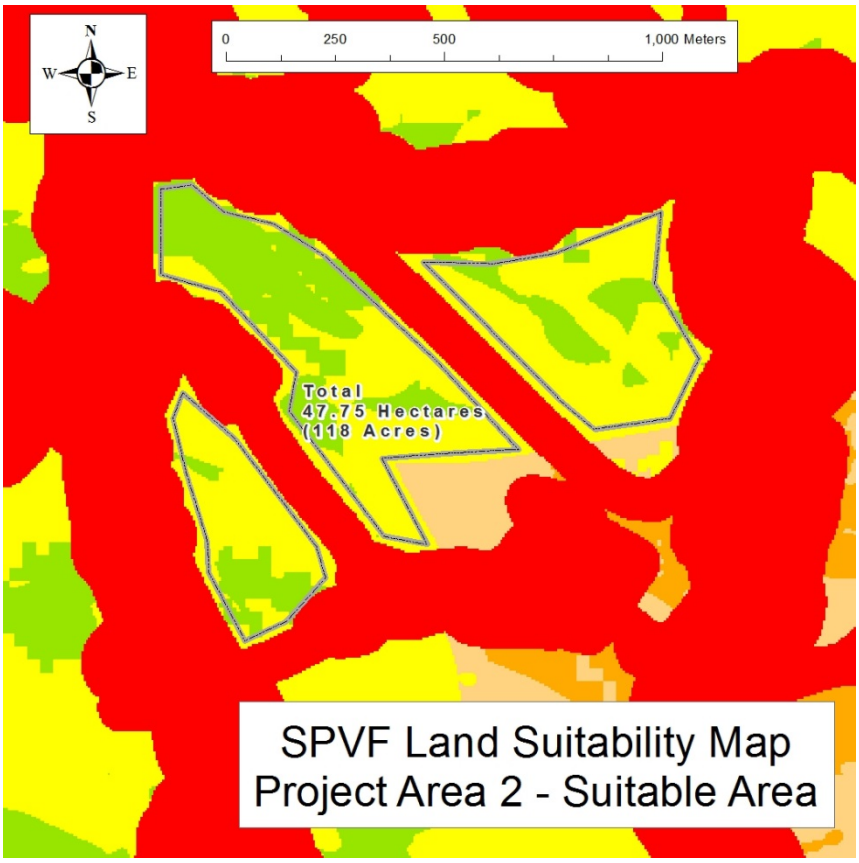

Fig. 4-17: Suitability of Project Area Two

Fig. 4-18 shows an aerial view of Project Area Two.

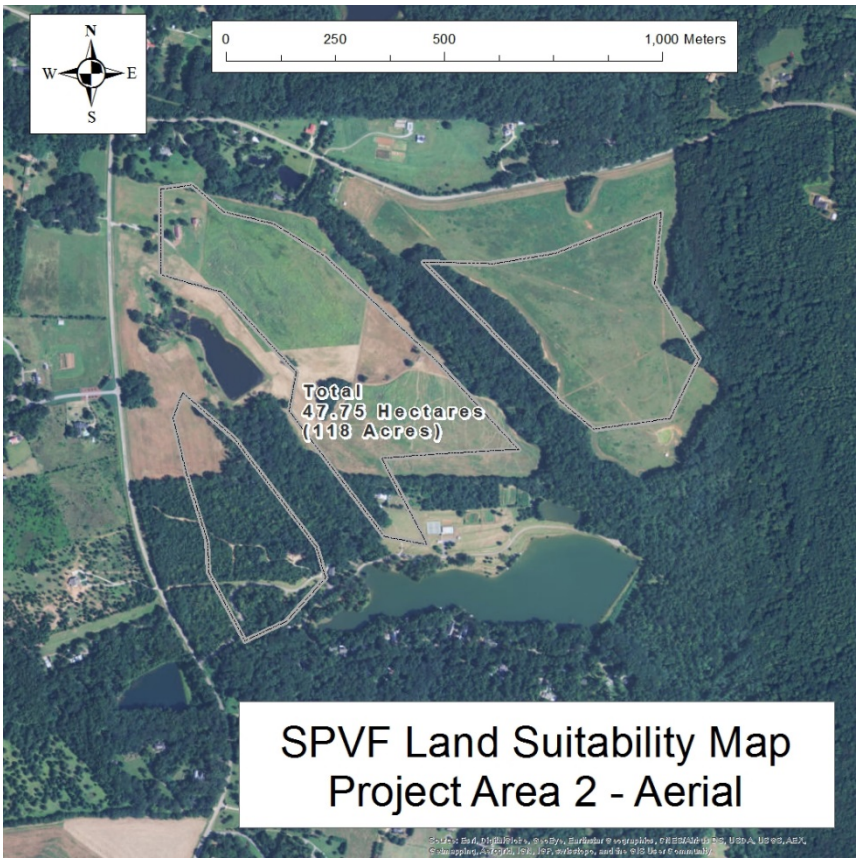

Fig. 4-18: Aerial of Project Area Two

Project Area Three is another example of a potential site that is large and continuous (Fig. 4-19). In this area, 40.47 Hectares (100 Acres) are identified as largely Best Suitability for a SVPF.

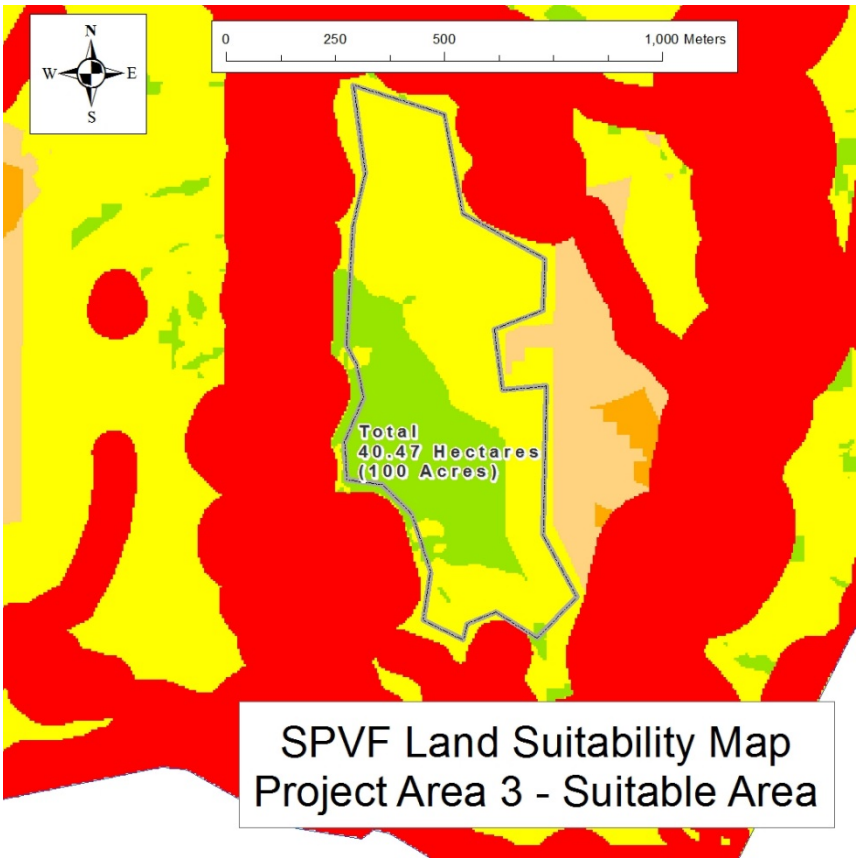

Fig. 4-19: Suitability of Project Area Three

An aerial of the area is shown in in Figure 4-20.

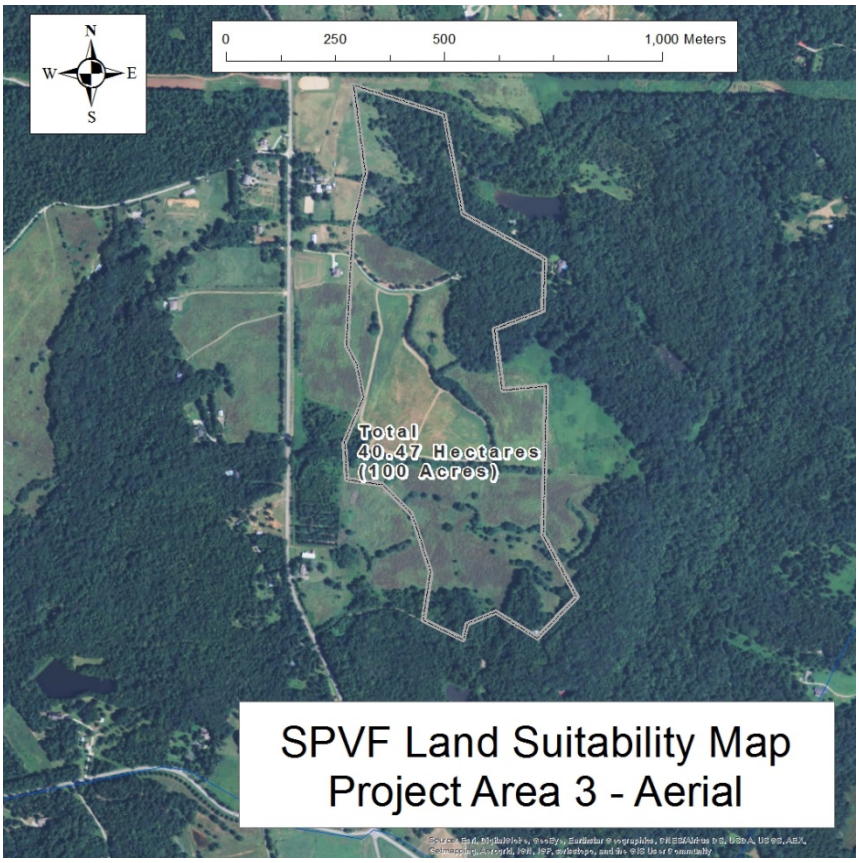

Fig. 4-20: Aerial of Project Area Three

The solar electric potential for these three project areas is summarized in Table 4-12.

Table 4-12: Project Area Solar Electric Potential

	Highly Suitable Area (Hectares)	Annual Electricity Potential (Mwh/Yr)	# of Potential Residences Supplied	Potential Billing at Current Rates ($)
Project Area 1	51.00	44,234	3,388	$5,069,178
Project Area 2	47.75	41,415	3,172	$4,746,142
Project Area 3	40.47	35,100	2,688	$4,022,542

Solar Potential for ACC

In order to get an idea of using the results from the analysis, polygon data of the top 10 sites of both the 10-meter and 1.22-meter Pass 1 constrained LSM maps were created. In isolating polygons of continuous "Most" and "Good" suitability, one gets an idea of the best areas in the county for SPVF development. The results are shown in Fig. 4-21.

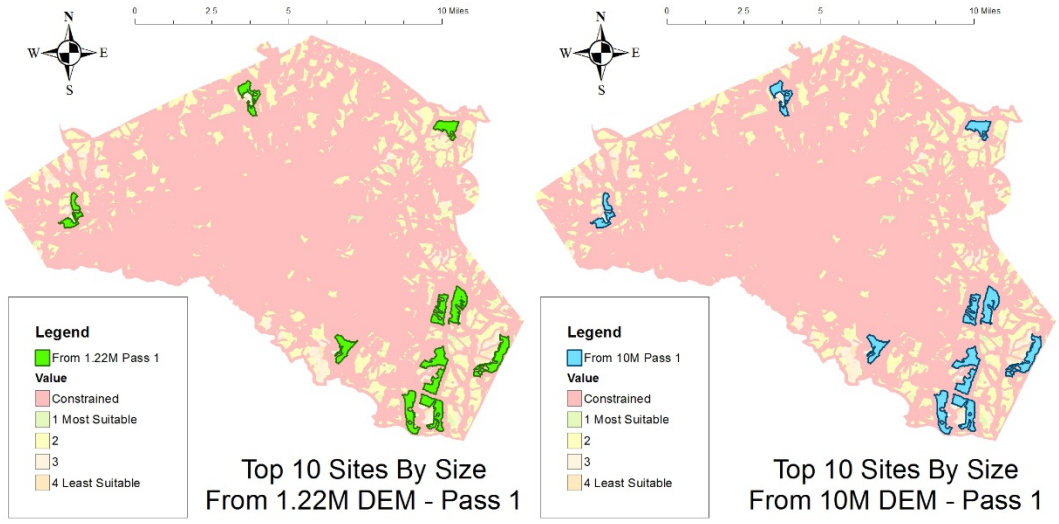

Fig. 4-21: Top 10 Sites from 10-M and 1.22-M LSM – Pass 1

The areas identified in this way are practically identical. The electric potential and economics of these Top 10 areas are shown in Table 4-13:

Table 4-13: ACC Top 10 Solar Sites Estimates

Largest Suitable Areas	Area (Ha)	Annual Electricity Produced (MWh/yr)	No. Avg. Residences Supplied	2013 Cost/MWh ($)	Potential Annual Income ($)	Installation Cost ($)
1	126.54	109752	8406	$114.60	$12,577,525	$156,340,170
2	103.21	89517	6856	$114.60	$10,258,624	$127,515,955
3	100.82	87444	6698	$114.60	$10,021,069	$124,563,110
4	99.87	86620	6634	$114.60	$9,926,643	$123,389,385
5	91.39	79265	6071	$114.60	$9,083,768	$112,912,345
6	68.97	59820	4582	$114.60	$6,855,318	$85,212,435
7	67.22	58302	4466	$114.60	$6,681,375	$83,050,310
8	66.38	57573	4410	$114.60	$6,597,883	$82,012,490
9	65.79	57061	4371	$114.60	$6,539,239	$81,283,545
10	65.58	56879	4357	$114.60	$6,518,366	$81,024,090
Total	**855.77**	**742232**	**56850**		**$85,059,810**	**$1,057,303,835**

These results suggest that by fully utilizing the top 10 sites in ACC at an installation cost of roughly one billion dollars would produce enough electrical power for all of the 51,259 housing units identified in ACC in 2013.

At the level of Pass 3, and just as was shown with the results shown in the map products and statistics, the increase in the weight of slope and aspect increases the differences between the results, as shown in Fig. 4-22.

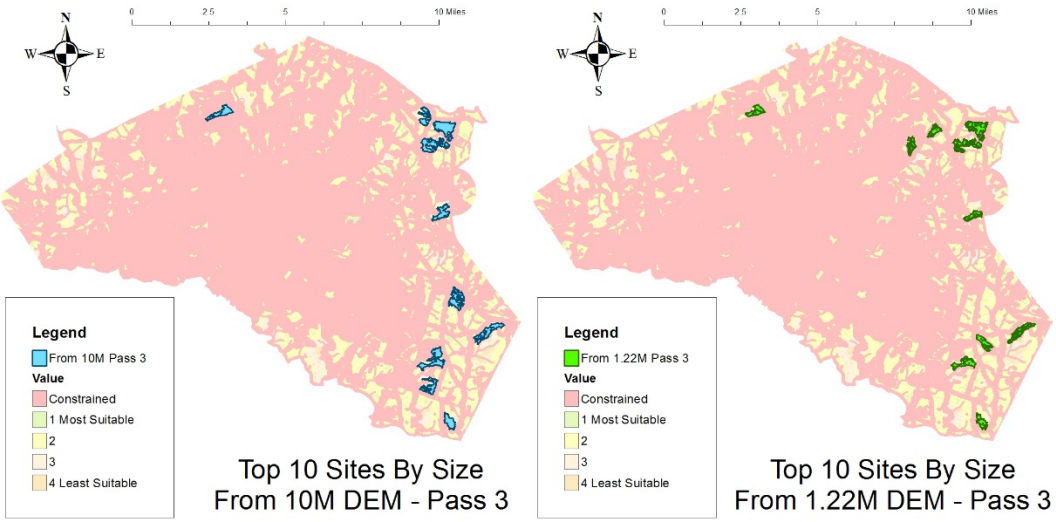

Fig. 4-22: Top 10 Sites from 10M and 1.22M LSM – Pass 3

While there is still some similarity in the areas identified at Pass 3, the differences are readily apparent. Another evidence that increasing the weight of slope and aspect in the model causes potential differences between the 10-meter and 1.22-meter results.

Clearly there is potential for huge amounts of clean energy to be produced in ACC, but what are the realities of the cost to install, maintain and secure an SPVF installation? Also, what are those realities in Georgia? These questions are explored below.

SPVF Installation & Maintenance

Innovative Solar Systems estimates the cost for installing SPVFs at $1,235,500/hectare ($500,000/acre) in the United States. If a solar project in ACC were to simply sell back the power produced to consumers at the same 2013 $114.60/MWh as the average electrical power consumer in GA pays, it would take nearly 12.5 years to pay for the installation. This does not include the Operations & Maintenance (O&M) cost over that

time, which Scott Madden Management Consultants estimates at $47,000 to $60,000/MW-yr (Jacobi, et al., 2010). In the Top 10 sites scenario, these O&M costs would increase the time for payoff of the installation to 16.23 to 17.73 years. Many areas have incentive programs in place to help with the upfront costs of solar installations at the residential and utility-scale level. There are some solar rebate and incentive programs active, at this time, in Georgia. One of these is the regional Solar Solutions Incentive from the Tennessee Valley Authority will grant $0.04 per kWh for 10 years in addition to the Renewable Standard Offer program. The Renewable Standard Offer plan is designed to help with small to mid-sized utility scale projects to purchase clean energies at a set price. Georgia Power has a Power Buyback Program that pays small to mid-sized utility scale projects currently $0.17 per kWh for their electric power. Programs such as these, combined with federal incentives, of which there are many programs, help to offset these high costs to initiate a solar project. Using the Database of State Incentives for Renewables and Efficiency, maintained by North Carolina State University's NC Clean Energy Technology Center, 43 active regulatory policies and incentive programs were identified for the ACC area.

CHAPTER 5

CONCLUSIONS

Expected Results

When the research on this project began, the initial expectation was that the result of the analysis process would be less than 5% different for data from a 10-meter DEM vs. a high-resolution product of 1.22-meter resolution. The results of this study show that when comparing the products of GIS-based MCDM processes for SPVF Site Suitability with geographic data derived from both high (1.22-meter) and low-resolution (10-meter) DEM data, the magnitude of the influence of the slope and aspect data determine the degree of deviation. The expected result of less than 5% deviation was found for the analysis where the total influence of the DEM-derived products was less than 20% of the model. This is greater than the total model influence values of DEM-derived data encountered in the literature; 10% (Uyan, 2003), 16% (Carrión, et al. 2008a; Sanchez-Lozano, et al., 2013). Even with an increasing statistical difference with that increased influence of slope and aspect, many areas determined to be Most Suitable in the final product are still visually defined. The main impact of high-resolution data and increased weight of the product is a "fuzziness" to the appearance of the suitability regions that, depending on the goal of the analysis (i.e., first-order, large area identification) may actually be negative.

Recommendation for Future Work

This project and its results have created quite a few questions which suggest future research. One of the first is to test at exactly which weight combination the slope and aspect value deviations introduced by the 10-meter data vs. the 1.22-meter data causes deviation in the LSM that passes a set threshold determined by the researcher to be where the two LSMs could not reasonable be considered similar. From this study, the determination was that an aspect and slope having a 10% total influence on the LSM produced two statistically similar LSM result. This was also the case with the 20% total influence. Future research could determine just where between 20% and 36% total influence that similarity degrades to the point of rendering the two datasets too dissimilar.

Along the same lines, one could see if this threshold is consistent among various geographic regions. While the less-than 20% value may be valid for the piedmont, what about mountainous areas? What about coasts? Further research could shed light on this. Should it be found that geographic region is not a factor of variation, and the slope and aspect should account for less than 20% total influence in a GIS-based MCDM process for SPVF site suitability analysis such as this project, it would be feasible to perform a nationwide analysis to identify regions of higher concentration of suitability using NED USGS 10-meter DEM data. When this sort of “first-pass” analysis is complete, areas that seem suitable for further analysis could be scheduled for a closer look.

A potential for future work with AHP weights is simple adjusting the influence of slope and aspect relative to each other. The literature suggests that slopes are more important

that aspect (Carrión, et al. 2008a; Sanchez-Lozano, et al., 2013), but some industry standards suggest otherwise.

Another consideration for future study is comparing the use of a DEM combined with LULC data to a Digital Surface Model (DSM) in estimating the shading effect of tree cover on a potential solar site. With a Lidar-derived DSM, one has a clear indication of canopy structure around a potential site and can reduce the site by the shading that would occur during the year. This could perhaps be estimated by using the LULC classification of "Forest" and applying a shading factor determined by the type of forest stand the LULC indicates. This could be a constraint layer for a future MCDM process.

Another important factor for future studies is best ways to represent appropriate electricity infrastructure to support a SPVF installation in an analysis such as this, where road centerline data of state highways and larger county roads was used as a proxy for high-capacity transmission lines and the assumption of near-by three-phase distribution. Utility providers do not typically readily release infrastructure data. In the literature, this criteria has a 30 to 40% influence on the total model (Uyan, 2003; Sanchez-Lozano, et al., 2013), so finding ways to approximate that important piece of the decision-making model for SPVFs is important.

Contribution of Project

There may very well be a day that nation-wide (and world-wide) coverage with high-resolution DEM data, or the capability with Unmanned Aircraft Systems (UAS)

to quickly and inexpensively obtain elevation data for almost any project scope, will render the specific results of this work somewhat obsolete, but the methodology established is sound for a variety of circumstances comparing the impact of resolution on MCDM-based site suitability surveys, whether they be 10-meter to 1.22-meter or 1-meter to .5-meter or beyond.

Summary

Producing electricity through utility-scale SPVFs is a clean, renewable source of power that is reducing in price and increasing in efficiency. When siting a SVPF, there are many factors to consider and it is beneficial to use GIS-based MCDM processes to help make those decision. When informing this analysis, one will want the best data available, but sometimes these data come with a significant price tag. This is the case with procuring high-resolution DEM data by Lidar survey. In this study, Land Suitability Maps were produced by conducting identical GIS-based MCDM processes informed first by data derived from 1.22-meter Lidar DEM data and then by using10-meter USGS NED DEM data. This MCDM process was modelled after a study encountered in the literature (Uyan, 2013). In this reproduction and comparison, the results were found to be statistically similar with a high correlation of 0.971 and a low normalized RMSD of 3.2%. When these were repeated with the importance of the DEM derived products increased, there was a marked decrease in correlation and increase in the deviation between them. The conclusion is that there is little statistical difference between the high and low-resolution LSM result of an MCDM process such as the AHP used in this study when the geographic characteristics criteria of aspect and slope are less than or equal to

approximately 20% of the total weight of the criteria used. Should the criteria of aspect and slope be more that 20% of the total weight of the decision-making process, there will certainly be a significant difference between the results one would get with the comparison of output from high vs. low-resolution DEM data. That being said, the visual difference in utilizing the resulting LSMs, even with the increased weights of the aspect and slope inputs, was low and many of the areas of best suitability were able to be visually identified in all of the LSMs. While having the high-resolution Lidar-derived DEM data to work from is useful, a viable LSM product can be produced from nationally available 10-meter NED DEM data as an input in to a SVPF Site Suitability Analysis using the AHP MCDM given the right influence of that data on the analysis.

REFERENCES

1. Adelaja, Soji et al. "Renewable energy potential on brownfield sites: A case study of Michigan." *Energy Policy* 38.11 (2010): 7021-7030.

2. Anderson, Eric S et al. "Horizontal resolution and data density effects on remotely sensed LIDAR-based DEM." *Geoderma* 132.3 (2006): 406-415.

3. Antonarakis, AS, Keith S Richards, and James Brasington. "Object-based land cover classification using airborne LiDAR." *Remote Sensing of Environment* 112.6 (2008): 2988-2998.

4. Aragonés-Beltrán, P et al. "An ANP-based approach for the selection of photovoltaic solar power plant investment projects." *Renewable and Sustainable Energy Reviews* 14.1 (2010): 249-264.

5. Bater, Christopher W, and Nicholas C Coops. "Evaluating error associated with lidar-derived DEM interpolation." *Computers & Geosciences* 35.2 (2009): 289-300.

6. Bazilian, Morgan et al. "Re-considering the economics of photovoltaic power." *Renewable Energy* 53 (2013): 329-338.

7. Birnie, Dunbar P. "Solar-to-vehicle (S2V) systems for powering commuters of the future." *Journal of Power Sources* 186.2 (2009): 539-542.

8. Bode, Collin A et al. "Subcanopy Solar Radiation model: Predicting solar radiation across a heavily vegetated landscape using LiDAR and GIS solar radiation models." *Remote Sensing of Environment* (2014).

9. Burger, Bruno “Electricity production from solar and wind in Germany in 2014". http://www.ise.fraunhofer.de/. Fraunhofer Institute, Germany. 2014-07-21. p. 5.

10. Calvert, K, Joshua M Pearce, and WE Mabee. "Toward renewable energy geo-information infrastructures: Applications of GIScience and remote sensing that build institutional capacity." *Renewable and sustainable energy reviews* 18 (2013): 416-429.

11. Carrión, J Arán et al. "Environmental decision-support systems for evaluating the carrying capacity of land areas: Optimal site selection for grid-connected photovoltaic power plants." *Renewable and Sustainable Energy Reviews* 12.9 (2008): 2358-2380.

12. Carrión, J Arán et al. "The electricity production capacity of photovoltaic power plants and the selection of solar energy sites in Andalusia (Spain)." *Renewable Energy* 33.4 (2008): 545-552.

13. Carswell, W.J., Jr., 2014, The 3D Elevation Program—Summary for Georgia: U.S. Geological Survey Fact Sheet 2014–3058, 2 p., *http://dx.doi.org/10.3133/fs20143058*

14. Caruso, V. "Standards for digital elevation models." *American Society for Photogrammetry and Remote Sensing (ASPRS) and American Congress on Surveying and Mapping (ACSM) annual convention proceedings* 1 Mar. 1987: 159-166.

15. Charabi, Yassine, and Adel Gastli. "PV site suitability analysis using GIS-based spatial fuzzy multi-criteria evaluation." *Renewable Energy* 36.9 (2011): 2554-2561.

16. Dehvari, Abdolhamid, and Richard John Heck. "Removing non-ground points from automated photo-based DEM and evaluation of its accuracy with LiDAR DEM." *Computers & Geosciences* 43 (2012): 108-117.

17. DiSavino, Scott. "MidAmerican's Giant California Solar Star Power Plant Enters Service." *Reuters*. Thomson Reuters, 10 Jan. 2014. Web. 26 Apr. 2015.

18. Fujii, Takashi, and Tetsuo Fukuchi. *Laser remote sensing*. Takashi Fujii & Tetsuo Fukuchi. CRC press, 2005.

19. Gastli, Adel, and Yassine Charabi. "Solar electricity prospects in Oman using GIS-based solar radiation maps." *Renewable and Sustainable Energy Reviews* 14.2 (2010): 790-797.

20. Goetzberger, Adolf, Christopher Hebling, and Hans-Werner Schock. "Photovoltaic materials, history, status and outlook." *Materials Science and Engineering: R: Reports* 40.1 (2003): 1-46.

21. Green, Martin A. "Photovoltaics: technology overview." *Energy Policy* 28.14 (2000): 989-998.

22. Haile, Alemseged Tamiru, and THM Rientjes. "Effects of LiDAR DEM resolution in flood modelling: a model sensitivity study for the city of Tegucigalpa, Honduras." *ISPRS WG III/3, III/4* 3 (2005): 12-14.

23. Hammer, Annette et al. "Solar energy assessment using remote sensing technologies." *Remote Sensing of Environment* 86.3 (2003): 423-432.

24. Heidemann, Hans Karl. "Lidar base specification version 1.0." *US Geological Survey Techniques and Methods* (2012): 63.

25. Hsiao, Lin-Hsuan, and Ke-Sheng Cheng. "Assessing Uncertainties in Accuracy of Landuse Classification Using Remote Sensing Images." *ISPRS-International Archives of the Photogrammetry, Remote Sensing and Spatial Information Sciences* 1.1 (2013): 19-23.

26. Hummel, Susan et al. "A comparison of accuracy and cost of LiDAR versus stand exam data for landscape management on the Malheur National Forest." *Journal of forestry* 109.5 (2011): 267-273.

27. Huang, JP, KL Poh, and BW Ang. "Decision analysis in energy and environmental modeling." *Energy* 20.9 (1995): 843-855.

28. Jacobi, Jere, and R. Starkweather. "Solar Photovoltaic Plant Operating and Maintenance Costs." *ScottMadden report September* (2010).

29. Janke, Jason R. "Multicriteria GIS modeling of wind and solar farms in Colorado." *Renewable Energy* 35.10 (2010): 2228-2234.

30. Joerin, Florent, Marius Thériault, and Andre Musy. "Using GIS and outranking multicriteria analysis for land-use suitability assessment." *International Journal of Geographical information science* 15.2 (2001): 153-174.

31. Kazmerski, Lawrence. "Best research cell efficiencies." *National Renewable Energy Laboratory* (2010).

32. Keating, T.J. et al. Solar Access Public Capital (SAPC) Working Group: Best Practices in PV Operations and Maintenance; Version 1.0, March 2015; Period of Performance, January 1, 2014 - December 31, 2015. Golden, CO, USA: National Renewable Energy Laboratory, 2015

33. Liang, Ruobing et al. "Performance evaluation of new type hybrid photovoltaic/thermal solar collector by experimental study." *Applied Thermal Engineering* 75 (2015): 487-492.

34. Makki, Adham, Siddig Omer, and Hisham Sabir. "Advancements in hybrid photovoltaic systems for enhanced solar cells performance." *Renewable and Sustainable Energy Reviews* 41 (2015): 658-684.

35. Malzewski, Jacek. "GIS-based land-use suitability analysis: a critical overview." *Progress in planning* 62.1 (2004): 3-65.

36. Malczewski, Jacek. "GIS-based multicriteria decision analysis: a survey of the literature." *International Journal of Geographical Information Science* 20.7 (2006): 703-726.

37. Malczewski, Jacek. "Ordered weighted averaging with fuzzy quantifiers: GIS-based multicriteria evaluation for land-use suitability analysis." *International Journal of Applied Earth Observation and Geoinformation* 8.4 (2006): 270-277.

38. Murphy, Paul NC et al. "Stream network modelling using lidar and photogrammetric digital elevation models: a comparison and field verification." *Hydrological Processes* 22.12 (2008): 1747-1754.

39. Myers, Daryl R. "Solar radiation modeling and measurements for renewable energy applications: data and model quality." *Energy* 30.9 (2005): 1517-1531.

40. Neal, Alan. "LiDAR Is Gaining Momentum." *Foresite Group*. Foresite Group, 03 Feb. 2015. Web. 26 Apr. 2015.

41. Nguyen, HT, and Joshua M Pearce. "Estimating potential photovoltaic yield with r. sun and the open source geographical resources analysis support system." *Solar Energy* 84.5 (2010): 831-843.

42. Ong, Sean et al. "Land-use requirements for solar power plants in the United States." *Retrieved December* 10 (2013): 2014.

43. Pearce, Joshua M. "Photovoltaics—a path to sustainable futures." *Futures* 34.7 (2002): 663-674.

44. Peng, Shouzhang, Chuanyan Zhao, and Zhonglin Xu. "Modeling Spatiotemporal Patterns Of Understory Light Intensity Using Airborne Laser Scanner (Lidar)." ISPRS Journal Of Photogrammetry & Remote Sensing 97.(2014): 195-203.Academic Search Complete. Web. 26 Jan. 2015.

45. Pereira, José MC, and Lucien Duckstein. "A multiple criteria decision-making approach to GIS-based land suitability evaluation." *International Journal of Geographical Information Science* 7.5 (1993): 407-424.

46. Perez, Richard et al. "A new operational model for satellite-derived irradiances: description and validation." *Solar Energy* 73.5 (2002): 307-317.

47. Pérez-Higueras, P et al. "High Concentrator PhotoVoltaics efficiencies: Present status and forecast." *Renewable and Sustainable Energy Reviews* 15.4 (2011): 1810-1815.

48. Rayburg, Scott, Martin Thoms, and Melissa Neave. "A comparison of digital elevation models generated from different data sources." *Geomorphology* 106.3 (2009): 261-270.

49. Renné, David S et al. *Solar resource assessment*. National Renewable Energy Laboratory, 2008.

50. Renslow, Michael S. "Manual of airborne topographic lidar." Michael S Renslow. 2012.

51. Ripley, Brian D. *Spatial Statistics*. Vol. 575. John Wiley & Sons, 2005.

52. Saaty, Thomas L. "How to make a decision: the analytic hierarchy process." *European journal of operational research* 48.1 (1990): 9-26.

53. Sánchez-Lozano, Juan M et al. "Geographical Information Systems (GIS) and Multi-Criteria Decision Making (MCDM) methods for the evaluation of solar farms locations: Case study in south-eastern Spain." *Renewable and Sustainable Energy Reviews* 24 (2013): 544-556.Varma,

54. Santos, T et al. "Applications of solar mapping in the urban environment." *Applied Geography* 51 (2014): 48-57.

55. Schwarz, Brent. "LIDAR: Mapping the world in 3D." *Nature Photonics* 4.7 (2010): 429-430.

56. Shi, Xun et al. "A comparison of LiDAR-based DEMs and USGS-sourced DEMs in terrain analysis for knowledge-based digital soil mapping." *Geoderma* 170 (2012): 217-226.

57. Solar Trade Association. "The STA 10 Commitments for Solar Farms - Solar Trade Association." Solar Trade Association. Solar Trade Association, 2 Mar. 2015. Web. 2 June 2015.

58. Sørensen, Bent. "GIS management of solar resource data." *Solar Energy Materials and Solar Cells* 67.1 (2001): 503-509.

59. Sørensen, Bent, and Peter Meibom. "GIS tools for renewable energy modelling." *Renewable Energy* 16.1 (1999): 1262-1267.

60. Stoms, David M, Stephanie L Dashiell, and Frank W Davis. "Siting solar energy development to minimize biological impacts." *Renewable Energy* 57 (2013): 289-298.

61. Sun, Yan-wei et al. "GIS-based approach for potential analysis of solar PV generation at the regional scale: A case study of Fujian Province." *Energy Policy* 58 (2013): 248-259.

62. Swanson, Richard M. "A vision for crystalline silicon photovoltaics." *Progress in photovoltaics: Research and Applications* 14.5 (2006): 443-453.

63. Uyan, Mevlut. "GIS-based solar farms site selection using analytic hierarchy process (AHP) in Karapinar region, Konya/Turkey." *Renewable and Sustainable Energy Reviews* 28 (2013): 11-17.

64. Vaze, Jai, Jin Teng, and Georgina Spencer. "Impact of DEM accuracy and resolution on topographic indices." *Environmental Modelling & Software* 25.10 (2010): 1086-1098.

65. Wade, Tasha, and Shelly Sommer. *A to Z GIS, An illustrated dictionary of geographic information systems*. ESRI press, 2006.

66. Wandinger, Ulla. *Introduction to lidar*. Springer New York, 2005.

67. Wehr, Aloysius, and Uwe Lohr. "Airborne laser scanning—an introduction and overview." *ISPRS Journal of Photogrammetry and Remote Sensing* 54.2 (1999): 68-82.

68. Yan, Wai Yeung, Ahmed Shaker, and Nagwa El-Ashmawy. "Urban land cover classification using airborne LiDAR data." Remote Sensing of Environment 158 (2015) 295-310

69. Yang, Ping et al. "What is the effect of LiDAR-derived DEM resolution on large-scale watershed model results?." *Environmental Modelling & Software* 58 (2014): 48-57.

70. Zhou, P, BW Ang, and KL Poh. "Decision analysis in energy and environmental modeling: An update." *Energy* 31.14 (2006): 2604-2622.

APPENDIX. AHP DEVELOPMENT DETAILS

With the Goal as the actual LSM products, the Objectives of the Goal are Environmental Factors and Economic Factors of that LSM. The environmental factors that those that are enforced by policy or aesthetics and primarily involve the question: “Is it in the public interest to place a SPVF at this location?” The economic factors are those that beg the question: “Is it financially practical to place an SVPF at this location?” The AHP comparison of these two Objectives applied too great a difference between them. With this being the case, a weighted, balanced comparison was performed where the same 1 to 9 by 1 scale was used but the comparison was direct with Environmental Factors scored as a 1 and Economic Factors scored a 2. This decision was based on the fact that policy restrictions represent a firm line on SVPF placement and, as a large component of the Environmental Factors, provide it a greater importance.

The Criteria of the Environmental Objective are Distance from Developed Areas and Land Use. In this study, Land Use was given greater importance to reflect the impact policy has on placement of SVPFs. The relative importance of each of these criteria are presented in Table A-1.

Table A-1: AHP Comparison for Environmental Objective

	Distance From Developed Areas	Land Use
Distance From Developed Areas	1	0.33
Land Use	3	1

The Sub-criteria of the Criteria for the Environmental Objective are:

Distance from Developed Areas – In order to minimize future development impact in the area of the SVPF and also mitigate the NIMBY effect, it is preferable to place a SVPF away from developed areas. The sub-criteria buffer zones established for this study are: less than 100 meters, 100 to 500 meters, 500 to 1000 meters and greater than 1000m. The areas less than 100 meters from a developed area are entirely unsuitable and therefore not even considered in the weighting process (weight value of 0). The relative importance of each of these sub-criteria are shown in Table A-2.

Table A-2: AHP Comparison for Distance from Developed Area Criteria

	100 to 500 meters	500 to 1000 meters	more than 1000 meters
100 to 500 meters	1	0.33	0.2
> 500 to 1000 meters	3	1	0.33
> 1000 meters	5	3	1

Land Use – Certain land use types are more appropriate for SVPFs than others. The land uses being considered are aggregated types explained, in detail, in the section on Data Processing and are: Barren Land, Shrubland, Herbaceous, Forest, Wetlands, Developed and Open Water. Some of the land use types in ACC are entirely unsuitable and therefore

not even considered in the weighting process (weight value of 0). The relative importance of each of the remaining sub-criteria are presented in Table A-3.

Table A-3: AHP Comparison for Land Use/Land Cover Criteria

	Barren	Shrubland	Herbaceous	Forest
Barren	1	2	3	7
Shrubland	0.5	1	3	6
Herbaceous	0.33	0.33	1	5
Forest	0.143	0.167	0.2	1

The Criteria of the Economic Objective are Distance from Transmission Lines, Distance from Roads, Aspect and Slope. A certain amount of ambiguity in the interpretation of the relative importance of these criteria provided an opportunity to test the impact of changes in the weights of our DEM-derived data (slope and aspect) within the Economic Objective on the similarity of the final land suitability maps generated from the 1.22-meter data vs. the 10-meter data. This was accomplished by performing an iteration of the entire project execution process for three iterations where the aspect and slope importance values were changed. Each of these iterations were referred to as “Passes”. In each of the passes, the slope and aspect remained of equal importance to each other, but changed in relation to the importance of the other criteria in the Economic Objective. For Pass 1, the slope and aspect have their lowest ranking of importance. The relative importance of each of these criteria are shown in Table A-4.

Table A-4: AHP Importance of Economic Objective – Pass 1

	Distance from Transmission Lines	Distance from Roads	Aspect	Slope
Distance from Transmission Lines	1	3	5	5
Distance from Roads	0.33	1	3	3
Aspect	0.2	0.33	1	1
Slope	0.2	0.33	1	1

For Pass 2, the slope and aspect have increased importance over Distance from Roads, but still remain equal to each other. The relative importance of each of these criteria are in Table A-5.

Table A-5: AHP Importance of Economic Objective – Pass 2

	Distance from Transmission Lines	Aspect	Slope	Distance from Roads
Distance from Transmission Lines	1	3	3	5
Aspect	0.33	1	1	3
Slope	0.33	1	1	3
Distance from Roads	0.2	0.33	0.33	1

For Pass 3, the slope and aspect have increased importance over Distance from Transmission Lines and Distance from Roads, but still remain equal to each other. The relative importance of each of these criteria are presented in Table A-6.

Table A-6: AHP Importance of Economic Objective – Pass 3

	Aspect	Slope	Distance from Transmission Lines	Distance from Roads
Aspect	1	1	2	4
Slope	1	1	2	4
Distance from Transmission Lines	0.5	0.5	1	3
Distance from Roads	0.25	0.25	0.33	1

The Sub-criteria of the Criteria for the Economic Objective are:

Distance from Transmission Lines – Of importance to the placement of SVPFs is the proximity of a potential sites to electric infrastructure sufficient to transmit the power generated. The farther a SVPF is from this infrastructure, the greater the cost of installation. The sub-criteria buffer zones established for this study are: less than 2000 meters, 2000 to 3000 meters, 3000 to 4000 meters and greater than 4000 meters. The relative importance of each of these sub-criteria are shown in Table A-7.

Table A-7: AHP Importance of Distance from Transmission Lines

	Less than 2000 meters	2000 to 3000 meters	3000 to 4000 meters	More than 4000 meters
Less than 2000 meters	1	5	7	9
2000 to 3000 meters	0.2	1	3	5
> 3000 to 4000 meters	0.143	0.33	1	3
> 4000 meters	0.11	0.2	0.33	1

Distance from Roads – While there is concern placing a SVPF too close to the road due to aesthetic or security reasons, there is also a concern on placing it too far from roads for

construction and maintenance cost reasons. The sub-criteria buffer zones established for this study are: less than 100 meters, 100 to 500 meters, 500 to 1000 meters and greater than 1000m. The areas less than 100 meters from roads are considered unsuitable and therefore not even considered in the weighting process (weight value of 0). The relative importance of each of the remaining sub-criteria are presented in Table A-8.

Table A-8: AHP Importance of Distance from Roads

	100 to 500 meters	500 to 1000 meters	More than 1000 meters
100 to 500 meters	1	3	5
> 500 to 1000 meters	0.33	1	3
> 1000 meters	0.2	0.33	1

Aspect – The direction a surface generally faces is important in that flat and southerly facing aspects have intrinsically better solar exposure. The sub-criteria are (bracketed for clarity): [Flat, S, SW or SE], [East], [West] and [North, NW, NE]. The relative importance of each of these sub-criteria are in Table A-9.

Table A-9: AHP Importance of Aspect

	Flat, S, SW or SE	East	West	North, NW, NE
Flat, S, SW or SE	1	5	5	9
East	0.2	1	1	5
West	0.2	1	1	5
North, NW, NE	0.11	0.2	0.2	1

Slope – Slope is an important factor in the siting of a SPVFs. Many developers of solar sites will place a cap of 10% on the slope of a site when considering a solar installation.

This varies, though, as methods have been developed to mitigate the negative effects of high slope. One such method is simply leveling the site, but that certainly can add to the cost of installation and may not be a best practice in developing the site. Low slopes are generally highly preferred. The values of the sub-criteria for this study are: less than 5%, 5 to 8%, 8 to 10%, 10 to 12% and greater than 12%. The areas more than 12% slope are considered unsuitable and therefore not even considered in the weighting process (weight value of 0). The relative importance of each of the remaining sub-criteria are indicated in Table A-10.

Table A-10: AHP Importance of Slope

	Less than 5%	5 to 8%	8 to 10%	10 to 12%
Less than 5%	1	3	5	7
5 to 8%	0.33	1	3	5
> 8 to 10%	0.2	0.33	1	3
> 10 to 12%	0.143	0.2	0.33	1